

# Fluctuations of the one-dimensional asymmetric exclusion process using random matrix techniques

T. Sasamoto \*

*Department of Mathematics and Informatics, Chiba University  
1-33 Yayoi-cho, Inage, Chiba, 263-8522, Japan*

October 26, 2018

## Abstract

The studies of fluctuations of the one-dimensional Kardar-Parisi-Zhang universality class using the techniques from random matrix theory are reviewed from the point of view of the asymmetric simple exclusion process. We explain the basics of random matrix techniques, the connections to the polynuclear growth models and a method using the Green's function.

## 1 Introduction

The one-dimensional asymmetric simple exclusion process (ASEP) [1, 2] is a stochastic process of many particles which perform asymmetric random walks with hardcore exclusion interaction. The ASEP is a simple model of statistical mechanical systems driven away from equilibrium [3, 4]. In spite of its simplicity, it shows a rich variety of phenomena and has attracted much attention. The stationary properties at a single time are already of great physical interest. A lot of insights have been obtained about the boundary induced phase transitions, the long range correlations and so on using the powerful matrix product method [5].

As for time dependent properties of the ASEP, the average behaviors are rather well described by the mean-field approximation. We can also understand some part of fluctuations from the fact that the ASEP belongs to the Kardar-Parisi-Zhang(KPZ) universality class of surface growth models [6–8]. In particular the critical exponents are understood by the dynamical renormalization method and can be confirmed by some exact solutions [9, 10].

---

\*email: sasamoto@math.s.chiba-u.ac.jp

In the past decade we have seen a substantial progress of understanding of this scaling behaviors of the 1D KPZ systems. In the language of the ASEP, a different approach based on a connection to the random matrix theory has been developed for the infinite system. It has allowed us to compute several time dependent quantities quite explicitly. Several important results and insights which have been obtained so far are (1) The fluctuations of the integrated current for several initial conditions have been computed and are shown to be equivalent to those of the largest eigenvalue of Gaussian ensembles. (2) The stationary two point correlation function has been computed explicitly. (3) The effects of boundary and initial conditions have been made quite explicit for certain special cases.

A problem is that these results are rather involved and often described in the language of random matrix theory. Moreover some results are stated from the point of view of other related models and the connection to the ASEP is not obvious. Hence for those who are not very familiar with random matrix theory and these models, the developments might look not easily accessible. The purpose of this article is to explain the basics of random matrix techniques and the relationship to a few of the related models. Some part of this paper will overlap with the paper by Prähofer and Spohn [11] which contains a lot of information on the same topic. The present article aims at giving some background knowledge for [12] and at the same time a collection of new results obtained after [12]. See also recent review papers on related topics [13–16].

The article is organized as follows. In the next section, we define the model. We mainly study the discrete time TASEP with parallel update scheme. The continuous time version is also considered. In section 3, we map the problem of current to a combinatorial one and get an expression in the form of multiple integrals. In section 4, the basics of the random matrix techniques are explained. The multi-point fluctuations are studied in section 5 by introducing the discrete polynuclear growth model and its multi-layer version. Some generalizations and variants are explained in section 6. In section 7, we explain another approach based on the Green’s function. The final section is devoted to the concluding remarks.

## 2 Models

In this article we mainly consider a discrete time TASEP (dTASEP) on the infinite lattice,  $\mathbb{Z}$ . There are several versions of the update schemes. Here we employ the parallel update for which the model is defined as follows. Each site of the lattice can be occupied by a particle or is empty (Fig. 1). Suppose that at each time step each particle tosses its own coin which shows heads with probability  $1 - q$ . If it turns out a head the particle tries to hop to the right neighboring site. If the target site is occupied, the hopping does not occur due to the exclusion interaction among particles. If it turns out a tail, on the other hand, the particle remains at the same site. This is the TASEP with parallel update. The parameter  $q$  here should not be confused with the asymmetry parameter in the partially ASEP which is often referred to as  $q$  in the study of ASEP.

The above definition describes how the configuration of the lattice changes as time goes

on. It is also possible to define the same process by focusing on when each particle makes jumps to the right. Notice that the distribution of the waiting time of each hopping after it becomes possible is geometrically distributed with parameter  $q$ . Suppose that each particle has its own clock instead of the coin. It rings after geometrically distributed time at which the particle tries to hop to the right neighboring site. If the target site is occupied, the hopping does not occur. This description of the process defines the same TASEP with parallel update as above.

The stationary measure with constant density  $\rho$  is rather simple. It is determined by the condition that the probability  $P(\eta_j, \eta_{j+1})$  that arbitrary consecutive two sites  $j, j+1$  are occupied ( $\eta_j = 1$ ) or empty ( $\eta_j = 0$ ) is given by [17]

$$P(00) = 1 - \rho - J/(1 - q), \quad (2.1)$$

$$P(01) = P(10) = J/(1 - q), \quad (2.2)$$

$$P(11) = \rho - J/(1 - q), \quad (2.3)$$

where  $J$  is the average current,

$$J = \frac{1}{2}(1 - \sqrt{1 - 4(1 - q)\rho(1 - \rho)}). \quad (2.4)$$

We remark that in the stationary state the waiting time of each particle before making a hop is geometrically distributed with parameter  $1 - J/\rho$ .

In the study of nonequilibrium systems, one of the most fundamental quantity is the current. Let  $N(t)$  be the number of particles which crossed the bond between sites 0 and 1 from time 0 through  $t$ . The average behavior is easily seen to be  $N(t) \sim Jt$ , or more precisely,

$$\lim_{t \rightarrow \infty} \frac{N(t)}{t} = J. \quad (2.5)$$

Hence the next step is to understand the fluctuation of this quantity. From the KPZ theory the exponent of the fluctuation is expected to scale as  $N(t) - Jt \sim O(t^{1/3})$ . The random matrix techniques allow us to compute even the scaling function. Note that the stationary measure is not enough to get such information.

There is an important limiting case;  $q \rightarrow 1$ . Since the hopping probability  $1 - q$  goes to zero, one has to rescale the time at the same time to take a meaningful limit. Let us consider the limit  $q \rightarrow 1, t \rightarrow \infty$  with  $\tilde{t} = (1 - q)t$  fixed. In this limit the process reduces to the continuous time TASEP (cTASEP) which is the most well studied in the study of ASEP [1,2]. In cTASEP during infinitesimal time duration  $dt$ , each particle tries to hop to the right neighboring site with probability  $dt$  under the same exclusion principle as for the discrete case. It is again possible to define the model using the waiting time for hoppings. The only difference as compared to the dTASEP is that each clock now rings after an exponential time with parameter one. A remark is in order. In the following, when the cTASEP is discussed, the time  $t$  should be understood as the rescaled time  $\tilde{t}$ .

The stationary measure of the cTASEP with density  $\rho$  is Bernoulli with parameter  $\rho$ , i.e., each site is independent and is occupied with probability  $\rho$  or is empty with probability  $1 - \rho$ . The average current is known to be  $J = \rho(1 - \rho)$ .

### 3 Combinatorial Approach

In this section we explain a result for the fluctuation of  $N(t)$  following [18]. The initial condition is taken to be the step one, in which all sites  $x \leq 0$  are occupied and all sites  $x > 0$  are empty at time 0 (Fig. 2). In this case one can label the particles from the right so that the particle  $j$  ( $j = 1, 2, \dots$ ) starts from site  $1 - j$ . Several results for other initial and boundary conditions will be explained in sections 6 and 7. We denote the measure corresponding to the ASEP dynamics by  $\mathbb{P}$ .

The first step in this approach is to introduce the “waiting time” table, or the matrix  $w = \{w_{i,j}\}$ , in which the  $(i, j)$  element  $w_{i,j}$  is the waiting time of the  $j$ th particle before making the  $i$ th hop after the target site becomes empty. Let us see the example in Fig. 3. The configuration does not change until the first particle moves to the site one. It took 1 step before the first move and hence  $w_{1,1} = 1$ . Now two particles can move to the right. It took 1 step (resp. 2 steps) before the second (resp. first) particle makes the first (resp. second) jump and hence  $w_{1,2} = 1$  (resp.  $w_{2,1} = 2$ ). After the second jump of the first particle the second particle waits 2 steps before the next move and hence  $w_{2,2} = 2$ . One continues this process to get all  $w_{i,j}$ ’s for a given sample of the dynamics of dTASEP. For this example the matrix looks like

$$w = \begin{bmatrix} 1 & 1 & 1 & 3 & \dots \\ 2 & 2 & 1 & 0 & \\ 1 & 0 & 0 & 1 & \\ 1 & 2 & 1 & 0 & \\ \vdots & & & & \ddots \end{bmatrix}. \quad (3.1)$$

It is clear that the time evolution of the dTASEP is equivalent to the infinite matrix  $w_{i,j}$ . If we call a matrix whose elements are nonnegative integers an  $\mathbb{N}$  matrix,  $w$  is an  $\mathbb{N}$  matrix. When considering various realizations of dynamics, each  $w_{i,j}$  is a random variable and geometrically distributed with parameter  $q$ ;  $\mathbb{P}(w_{i,j} = l) = (1 - q)q^l$  ( $l = 0, 1, 2, \dots$ ).

Next let us define  $G(M, N)$  by

$$G(M, N) = \max_{\pi \in \Pi_{M,N}} \left\{ \sum_{(i,j) \in \pi} w_{i,j} \right\}. \quad (3.2)$$

Here  $\pi$  is a path from  $(1, 1)$  to  $(M, N)$  which consists of elementary path connecting points  $(i, j) \rightarrow (i + 1, j)$  or  $(i, j) \rightarrow (i, j + 1)$ . In the matrix representation as in (3.1),  $\pi$  is a down/right path, i.e., it starts from  $(1, 1)$  and goes either down or right until it reaches  $(M, N)$ .  $\Pi_{M,N}$  is the collection of all such paths. If we regard  $w_{i,j}$  as representing a value of a potential energy at a position  $(i, j)$ , (3.2) can be considered as the problem of the zero temperature directed polymer in random medium. One can confirm oneself that  $G(M, N) + M + N - 1$  is equal to the time at which the  $N$ th particle has just made the  $M$ th step. Considering the dynamics of the  $N$ th particle, one notices that  $N(t) \geq N$  is equivalent to saying that the  $N$ th particle makes the  $N$ th jump before  $t$ . Hence we have

$$\mathbb{P}[N(t) \geq N] = \mathbb{P}[G(N, N) + 2N - 1 \leq t]. \quad (3.3)$$

Though  $w$  is in principle an infinite matrix, to study  $N(t)$ , we can restrict our attention to the  $N \times N$  submatrix  $\{w_{i,j}\}_{1 \leq i,j \leq N}$  of  $w$ . This is related to the Markov property and the fact that in the TASEP each particle can not affect the dynamics of the particles on its right. For instance, from the  $3 \times 3$  submatrix of  $w$ ,

$$\begin{bmatrix} 1 & 1 & 2 \\ 2 & 2 & 1 \\ 1 & 0 & 0 \end{bmatrix}, \quad (3.4)$$

one sees that  $G(3,3) = 6$  with the maximizing path,  $(1,1) \rightarrow (2,1) \rightarrow (2,2) \rightarrow (2,3) \rightarrow (3,3)$ . This gives  $G(3,3) + 5 = 11$  which agrees with the time at which the third particle has made the third hop in Fig. 3.

To proceed we use a bijection known as the Robinson-Schensted-Knuth(RSK) algorithm between an  $\mathbb{N}$  matrix and a pair  $(P, Q)$  of semistandard Young tableaux(SSYT). A short explanation about the SSYT and the Schur function is given in the appendix. For more details and the RSK algorithm, see for instance [19,20]. The pair of SSYTs corresponding to (3.4) is

$$P = \begin{array}{|c|c|c|c|c|c|} \hline 1 & 1 & 1 & 1 & 2 & 3 \\ \hline 2 & 2 & & & & \\ \hline 3 & & & & & \\ \hline \end{array}, \quad Q = \begin{array}{|c|c|c|c|c|c|} \hline 1 & 1 & 1 & 2 & 2 & 2 \\ \hline 2 & 2 & & & & \\ \hline 3 & & & & & \\ \hline \end{array}.$$

In the language of SSYT, the  $G(N, N)$  is given by

$$G(N, N) = \lambda_1 \quad (3.5)$$

where  $\lambda_1$  is the length of the first row of  $P$ . This is easily seen as a property of the RSK algorithm. For our example,  $\lambda_1 = 6$  is the same as  $G(3,3)$ . Therefore the problem of  $N(t)$  is reduced to a combinatorial problem of SSYTs. If we denote the number of SSYT of shape  $\lambda$  and entries from  $\{1, 2, \dots, N\}$  by  $L(\lambda, N)$ , we have

$$\begin{aligned} \mathbb{P}[G(N, N) + 2N - 1 \leq t] &= (1 - q)^{N^2} \sum_{\lambda: \lambda_1 \leq t - 2N + 1} q^{|\lambda|} L(\lambda, N)^2 \\ &= (1 - q)^{N^2} \sum_{\lambda: \lambda_1 \leq t - 2N + 1} q^{|\lambda|} s_\lambda(\underbrace{1, \dots, 1}_N, 0, \dots)^2 \end{aligned} \quad (3.6)$$

where a formula (A.4) is used in the second equality. Rewriting (3.6) using the formula (A.6) and  $h_j = \lambda_1 - j + 1$ , one obtains

$$\mathbb{P}[G(N, N) + 2N - 1 \leq t] = \frac{1}{Z} \sum_{h_j = -N + 1}^{t - 2N + 1} \prod_{1 \leq j < l \leq N} (h_j - h_l)^2 \prod_{j=1}^N q^{h_j}. \quad (3.7)$$

Here and in the following the symbol  $Z$  is used to represent a normalization constant. For the present case it is

$$Z = \frac{q^{\frac{1}{2}N(N-1)}}{(1 - q)^{N^2}} \prod_{j=1}^N j!(j - 1)!. \quad (3.8)$$

The expression of the RHS of (3.7) has a strong similarity with a quantity appearing in the random matrix theory. Hence generalizing and applying techniques from random matrix theory, one can study the asymptotic behavior of the quantity to obtain

$$\lim_{N \rightarrow \infty} \mathbb{P} \left[ \frac{G(N, N) - \frac{2\sqrt{q}}{1-\sqrt{q}}N}{dN^{1/3}} \leq s \right] = F_2(s) \quad (3.9)$$

with  $d = q^{1/6}(1 + \sqrt{q})^{1/3}(1 - \sqrt{q})^{-1}$ . In terms of  $N(t)$ , this is equivalent to

$$\lim_{t \rightarrow \infty} \mathbb{P} \left[ \frac{N(t) - \frac{1-\sqrt{q}}{2}t}{d't^{1/3}} \geq -s \right] = F_2(s) \quad (3.10)$$

with  $d' = 2^{-4/3}q^{1/6}(1 - q)^{1/3}$ . The function  $F_2$  appearing on the RHS is called the GUE Tracy-Widom distribution function [21] and describes the distribution of the largest eigenvalue of the Gaussian unitary ensemble (GUE). Hence the above equation states that the current of the TASEP for the step initial condition is, in the appropriate scaling limit, equivalent to that of the largest eigenvalue of the GUE. It is stressed that  $F_2(s)$  is completely different from the error function which is the distribution function for the ordinary Gaussian fluctuation. This is the most basic and fundamental result in the approach of random matrix theory to the ASEP. Basics of random matrix techniques to obtain  $F_2$  and related quantities will be given in the next section.

Before ending the section, let us consider the cTASEP limit. In this limit,  $w_{i,j}$  becomes an exponential random variable with parameter one and (3.7) reduces to

$$\mathbb{P}[G(N, N) \leq t] = \frac{1}{Z} \int_{[0,t]^N} \prod_{1 \leq j < l \leq N} (x_j - x_l)^2 \prod_{j=1}^N e^{-x_j} dx \quad (3.11)$$

with

$$Z = \prod_{j=1}^N j!(j-1)!. \quad (3.12)$$

The same quantity appears in the random matrix theory as the distribution of the largest eigenvalue in an ensemble called the Laguerre unitary ensemble. As a result, for the cTASEP, we have

$$\lim_{t \rightarrow \infty} \mathbb{P} \left[ \frac{N(t) - \frac{t}{4}}{2^{-4/3}t^{1/3}} \geq -s \right] = F_2(s). \quad (3.13)$$

## 4 Random matrix techniques

In this section, we explain the basics of the techniques from random matrix theory which would be helpful to understand the results for the ASEP. In physics the random matrices were first introduced to model a complex Hamiltonian of nuclei. But the random matrix

theory has also found a lot of applications not only in nuclear physics but also in other branches of physics, mathematics, statistics and so on. The basic reference of random matrix theory is [22]. The book by Forrester [23] is also very useful.

A random matrix is a matrix with random elements. There are infinitely many variety of random matrix ensembles but there are some random matrix ensembles with especially good properties. Among them are the Gaussian ensembles which are defined by the probability distribution of  $N \times N$  matrices,

$$P(H)dH = e^{-\frac{\beta}{2}\text{Tr}H^2} dH. \quad (4.1)$$

Here  $\beta$  takes three different values  $\beta = 1, 2, 4$ . When  $\beta = 1$ ,  $H$  is taken to be a real symmetric matrix and  $dH = \prod_{j=1}^N dH_{jj} \prod_{j<l} dH_{jl}$ . Writing down the Tr in (4.1) explicitly, one sees that this definition is equivalent to saying that each independent element obeys a Gaussian distribution with variance 1 for the diagonal and 1/2 for the off-diagonal elements. This ensemble is called the Gaussian orthogonal ensemble(GOE). For  $\beta = 2$ ,  $H$  is taken to be a Hermitian matrix and  $dH = \prod_{j=1}^N dH_{jj} \prod_{j<l} dH_{jl}^R dH_{jl}^I$  where  $H_{jl}^R$  and  $H_{jl}^I$  are the real and imaginary parts of  $H_{jl}$  respectively. This is the Gaussian unitary ensemble (GUE). For  $\beta = 4$ , the ensemble is called the Gaussian symplectic ensemble (GSE). For this case,  $H$  is taken to be a self-dual quaternion matrix, whose definition is not given here.

In many applications we are interested in the statistics of eigenvalues. For the Gaussian ensembles, we can derive the joint density function for eigenvalues explicitly. Basically we change the coordinate from the original matrix elements to the eigenvalues and the diagonalizing matrix and then integrate out the latter degrees of freedom. The procedure is explained in [22, 23] but is omitted here since it is not directly used in the applications to ASEP. The resulting joint probability density function of eigenvalues  $\{x_j\}_{j=1,\dots,N}$  is

$$P_{N\beta}(x_1, \dots, x_N) = \frac{1}{Z} \prod_{1 \leq j < l \leq N} |x_j - x_l|^\beta \prod_{j=1}^N e^{-\beta x_j^2/2} \quad (4.2)$$

for  $\beta = 1, 2, 4$ . Let  $\mathbb{P}_{N\beta}$  denote the corresponding measure. Using this expression one can study in principle any statistical property of eigenvalues of the Gaussian ensembles. Here we focus on the statistical behavior of the largest eigenvalue. From the joint eigenvalue distribution (4.2), the probability that the largest eigenvalue  $x_1$  is less than  $u$  is given by

$$\mathbb{P}_{N\beta}[x_1 \leq u] = \frac{1}{Z} \int_{(-\infty, u]^N} \prod_{1 \leq j < l \leq N} |x_j - x_l|^\beta \prod_{j=1}^N e^{-\beta x_j^2/2} dx_j. \quad (4.3)$$

Next for the case of  $\beta = 2$  we rewrite this expression to another which is more suitable for asymptotic analysis. The probability density (4.2) for  $\beta = 2$  can be written as

$$\frac{1}{Z} \det(\varphi_j(x_l))_{j,l=1}^N \det(\psi_j(x_l))_{j,l=1}^N \quad (4.4)$$

if we notice

$$\prod_{1 \leq j < l \leq N} (x_l - x_j) = \det(x_j^{l-1})_{j,l=1}^N, \quad (4.5)$$

and set  $\varphi_j(x) = \psi_j(x) = x^{j-1}e^{-x^2/2}$ . We show the identity

$$\frac{1}{Z} \int_{-\infty}^{\infty} dx \det(\varphi_j(x_l))_{j,l=1}^N \det(\psi_j(x_l))_{j,l=1}^N \prod_{j=1}^N (1 + g(x_j)) = \det(1 + Kg). \quad (4.6)$$

Here the determinant on the RHS is the Fredholm determinant defined as

$$\det(1 + Kg) = \sum_{m=0}^{\infty} \frac{(-1)^m}{m!} \int_{-\infty}^{\infty} dx_1 \cdots \int_{-\infty}^{\infty} dx_m g(x_1) \cdots g(x_m) \det(K(x_j, x_l))_{j,l=1}^m, \quad (4.7)$$

where the kernel is

$$K(x_1, x_2) = \sum_{j,l=1}^N \psi_j(x_1) [A^{-1}]_{j,l} \varphi_l(x_2) \quad (4.8)$$

with the matrix  $A$  being

$$A_{j,l} = \int_{-\infty}^{\infty} dx \varphi_j(x) \psi_l(x). \quad (4.9)$$

There are several ways of proof; here we follow [24]. Using the Heine identity,

$$\int dx_1 \cdots \int dx_N \det(\varphi_j(x_l))_{j,l=1}^N \det(\psi_j(x_l))_{j,l=1}^N = \det\left(\int dx \varphi_j(x) \psi_l(x)\right)_{j,l=1}^N, \quad (4.10)$$

the LHS of (4.6) can be rewritten as

$$\begin{aligned} & \det(A_{j,l} + \int dx \varphi_j(x) \psi_l(x) g(x)) / \det A \\ &= \det(1_{j,l} + \int dx (A^{-1} \varphi)_j(x) g(x) \cdot \psi_l(x)), \end{aligned} \quad (4.11)$$

where  $1$  is the identity matrix of size  $N$ . One can regard this as  $\det(1 + BC)$  if we set

$$B_{j,x} = (A^{-1} \varphi)_j(x) g(x), \quad C_{x,j} = \psi_j(x). \quad (4.12)$$

Then using a simple identity  $\det(1 + BC) = \det(1 + CB)$  and rewriting  $B, C$  again in terms of  $\varphi, \psi$ , we get (4.6). Some manipulations here are rather formal but can be justified [24]. Since (4.3) with  $\beta = 2$  is written in the form of LHS of (4.6) with  $g(x) = -\chi_{(u,\infty)}(x)$  where  $\chi_{(u,\infty)}(x) = 1(x > u), 0(x \leq u)$ , the probability that the largest eigenvalue  $x_1$  is less than  $u$  in the GUE is written in the form of the Fredholm determinant,

$$\mathbb{P}_{N2}[x_1 \leq u] = \det(1 + Kg). \quad (4.13)$$

To proceed, a nontrivial task is the computation of the inverse matrix  $A^{-1}$ . For the GUE, this is (implicitly) done as follows. Let us remember that the addition of a row or a column to another does not change the value of the determinant. Then the functions  $\varphi_j$  and  $\psi_j$  in (4.4), which we have taken to be the monic polynomials  $x^{j-1}$ , can be replaced

by any polynomials of the same degree modulo a numerical factor. For the GUE, it is convenient to take

$$\varphi_j(x) = \psi_j(x) = e^{-x^2/2} H_j(x) \quad (4.14)$$

where  $H_n(x)$  is the Hermite polynomials [25],

$$H_n(x) = (-1)^n e^{x^2} \frac{d^n}{dx^n} e^{-x^2}. \quad (4.15)$$

Using the orthogonality relation of the Hermite polynomials, one sees that  $A$  is diagonal,

$$A_{j,l} = \int_{-\infty}^{\infty} H_j(x) H_l(x) e^{-x^2} dx = \sqrt{\pi} 2^j j! \delta_{jl}. \quad (4.16)$$

Then the kernel (4.8) for the GUE, which we denote by  $K_{N2}(x_1, x_2)$ , is calculated to be

$$K_{N2}(x_1, x_2) = e^{-\frac{1}{2}(x_1^2 + x_2^2)} \sum_{n=0}^{N-1} \frac{H_n(x_1) H_n(x_2)}{\sqrt{\pi} 2^n n!}. \quad (4.17)$$

This expression of the kernel allows one to study various statistical properties of the eigenvalues such as the eigenvalue density, the two point correlation function, etc. To take a scaling limit for the largest eigenvalue, we use the asymptotic expression of the Hermite polynomial [26],

$$e^{-\frac{1}{2}x^2} H_n(x) \sim \pi^{\frac{1}{4}} 2^{(2n+1)/4} (n!)^{1/2} n^{-1/12} \text{Ai}(2^{1/2} n^{1/6} (x - \sqrt{2n})), \quad (4.18)$$

where  $\text{Ai}(x)$  is the Airy function defined by

$$\text{Ai}(x) = \frac{1}{2\pi} \int_{-\infty+i\epsilon}^{\infty+i\epsilon} e^{izx + \frac{i}{3}z^3} dz \quad (4.19)$$

with  $\epsilon > 0$ . If we set  $x_j = \sqrt{2N} + \xi_j / (\sqrt{2}N^{1/6})$  ( $j = 1, 2$ ), one has for large  $N$

$$K_{N2}(x_1, x_2) \sim \sqrt{2}N^{1/6} \mathcal{K}_2(\xi_1, \xi_2) \quad (4.20)$$

where

$$\mathcal{K}_2(\xi_1, \xi_2) = \frac{\text{Ai}(\xi_1)\text{Ai}'(\xi_2) - \text{Ai}(\xi_2)\text{Ai}'(\xi_1)}{\xi_1 - \xi_2} \quad (4.21)$$

is known as the Airy kernel. Hence one obtains

$$\lim_{N \rightarrow \infty} \mathbb{P}_{N2} \left[ (x_1 - \sqrt{2N})\sqrt{2}N^{1/6} \leq s \right] = \det(1 + \mathcal{K}_2 \mathcal{G}) =: F_2(s). \quad (4.22)$$

The function  $F_2(s)$  is defined as the Fredholm determinant (4.7) with the kernel  $\mathcal{K}_2$  (4.19) and  $\mathcal{G}(x) = -\chi_{(s, \infty)}$ . The function  $F_2(s)$  describes the fluctuation of the largest eigenvalue of GUE in the scaling limit and is called the GUE Tracy-Widom distribution function. It is known to have a different representation using the solution to the Painlevé II equation [21].

Equation (4.22) says that the largest eigenvalue  $x_1$  in the GUE behaves like  $x_1 \sim \sqrt{2N}$  in average, has a fluctuation of order  $O(N^{-1/6})$  and has the  $F_2$  as the distribution function in the  $N \rightarrow \infty$  limit if appropriately scaled.

The function  $F_2(s)$  is the same as the one which appeared in the RHS of (3.9) and (3.10). Notice a close similarity between (3.7) and (4.3) with  $\beta = 2$ . The main difference in (3.7) is that the Gaussian  $e^{-x^2}$  ( $x \in \mathbb{R}$ ) is replaced by  $q^h$  ( $h = 0, 1, 2, \dots$ ). As a consequence we use the orthogonal polynomials which are orthogonal with respect to the weight  $q^h$ , which is known as the Meixner polynomials [27]. Then (3.7) could be called the Meixner ensemble representation for the current of the TASEP. The derivation of (3.9) from (3.7) is more involved but is similar to the one for the GUE [18].

For GOE( $\beta = 1$ ) and GSE( $\beta = 4$ ) the power of the determinant in (4.3) is different from 2 and the above calculation does not work. But it is possible to modify the arguments and obtain analogous results [24, 28]. They read

$$\lim_{N \rightarrow \infty} \mathbb{P}_{N\beta} \left[ (x_1 - \sqrt{2N})\sqrt{2}N^{1/6} \leq s \right] = F_\beta(s) \quad (4.23)$$

with  $\beta = 1, 4$ . The functions  $F_1(s)$  (resp.  $F_4(s)$ ) is called the GOE (resp. GSE) Tracy-Widom distribution function. They are expressed as Fredholm determinants with  $2 \times 2$  matrix kernel. The Painlevé II representation is also known [28].

A remark is in order. To compare the results of ASEP with those of the Gaussian ensembles, it is sometimes more convenient to change the normalization from (4.1) to

$$P(H)dH = e^{-\frac{\beta}{4N} \text{Tr}H^2} dH. \quad (4.24)$$

Then (4.22) and (4.23) are replaced by

$$\lim_{N \rightarrow \infty} \mathbb{P}_{N\beta} \left[ \frac{x_1 - 2N}{N^{1/3}} \leq s \right] = F_\beta(s) \quad (4.25)$$

for  $\beta = 1, 2, 4$  in which the exponents of  $N$  are the same as in (3.9).

Let us now consider a time dependent version of the random matrix ensemble known as the Dyson's Brownian motion [29]. The random matrix  $H(t)$  now depends on time  $t$ . Each independent component of the matrix performs the Ornstein-Uhlenbeck process for which the Fokker-Plank equation for the probability density  $p(t, x)$  takes the form,

$$\frac{\partial}{\partial t} p(t, x) = D \frac{\partial^2}{\partial x^2} p(t, x) + \frac{\partial}{\partial x} (xp(t, x)). \quad (4.26)$$

Here  $D$  is the diffusion constant and should be taken appropriately depending on the ensembles in question. Let us consider the stochastic dynamics of the eigenvalues of this random matrix. We are interested in the multi-time joint distribution of the eigenvalues. It is known that, for general  $\beta$ , time evolution of the probability density of the eigenvalues is described by an equation which can be mapped to the quantum Calogero model [23]. For the GUE( $\beta = 2$ ) case, the system is a free fermion and we can get detailed information

from this fact as we see below. For the GOE( $\beta = 1$ ) and the GSE( $\beta = 4$ ), however, the analysis becomes much more involved and the computation of correlation functions have so far been very restricted.

Let us consider the stationary situation for the GUE in which the dynamics and the initial conditions are both taken to be the GUE type. We call this the tGUE (This is *not* a standard notation). If we denote the eigenvalues of the matrix  $H_{j,l}(t)$  by  $x_j^t$  ( $j = 1, 2, \dots, N$ ), the dynamics of them look like Fig. 4. The joint density function at two times can be written as a product of determinants,

$$P(x_1^{t_1}, \dots, x_N^{t_1}, x_1^{t_2}, \dots, x_N^{t_2}) = \frac{1}{Z} \det(\varphi_j^{(t_1)}(x_l^{t_1}))_{j,l=1}^N \cdot \det(\phi_{t_1, t_2}(x_j^{t_1}, x_l^{t_2}))_{j,l=1}^N \cdot \det(\psi_j^{(t_2)}(x_l))_{j,l=1}^N \quad (4.27)$$

where  $\varphi_j^{(t_1)}(x) = \psi_j^{(t_2)}(x) = e^{-x^2/2} x^{j-1}$  ( $j = 1, 2, \dots, N$ ) and

$$\phi_{t_1, t_2}(x_1, x_2) = \frac{1}{\sqrt{(1 - e^{-2(t_2 - t_1)})\pi}} \exp \left[ -\frac{(x_2 - e^{-(t_2 - t_1)} x_1)^2}{1 - e^{-2(t_2 - t_1)}} \right]. \quad (4.28)$$

This is a generalization of (4.4) to the two time case. The derivation can be found in [22, 23] but is omitted here since it is again not directly used in the applications to ASEP. Furthermore the joint probability that the largest eigenvalue  $x_1^{t_j}$  (the height of the top curve at  $t_j$  in Fig. 4) is less than  $u_j$  at time  $t_j$  ( $j = 1, 2$ ) is again given by a Fredholm determinant. Let us introduce a matrix

$$A_{jl} = \int_{-\infty}^{\infty} dx_1 \int_{-\infty}^{\infty} dx_2 \varphi_j^{(t_1)}(x_1) \phi_{t_1, t_2}(x_1, x_2) \psi_l^{(t_2)}(x_2), \quad (4.29)$$

and

$$\varphi_j^{(t_2)}(x_2) = \int_{-\infty}^{\infty} dx_1 \varphi_j^{(t_1)}(x_1) \phi_{t_1, t_2}(x_1, x_2), \quad (4.30)$$

$$\psi_j^{(t_1)}(x_1) = \int_{-\infty}^{\infty} dx_2 \phi_{t_1, t_2}(x_1, x_2) \psi_j^{(t_2)}(x_2). \quad (4.31)$$

Then we have

$$\mathbb{P}_{N2}[x_1^{t_1} \leq u_1, x_1^{t_2} \leq u_2] = \det(1 + K_{N2}g) \quad (4.32)$$

where the kernel is

$$K_{N2}(t_1, x_1; t_2, x_2) = \tilde{K}_{N2}(t_1, x_1; t_2, x_2) - \phi_{t_1, t_2}(x_1, x_2), \quad (4.33)$$

$$\tilde{K}_{N2}(t_1, x_1; t_2, x_2) = \sum_{j,l=1}^N \psi_j^{(t_1)}(x_1) [A^{-1}]_{jl} \varphi_l^{(t_2)}(x_2), \quad (4.34)$$

$$g(t_j; x) = -\chi_{(u_j, \infty)}(x), \quad (j = 1, 2), \quad (4.35)$$

with the convention that  $\phi_{t_1, t_2}(x_1, x_2) = 0$  when  $t_1 \geq t_2$ . In this kernel  $(t_1, t_2)$  should be understood as a representative of either  $(t_1, t_1)$ ,  $(t_1, t_2)$ ,  $(t_2, t_1)$ ,  $(t_2, t_2)$ . Similar abuse of

notation will be used in rest of the paper as well. The formula (4.32) can be derived by a generalization of the argument to get (4.6).

For the tGUE, the matrix  $A$  in (4.29) is again diagonalized by taking  $\varphi_j^{(t_1)}$  and  $\psi_j^{(t_2)}$  to be the Hermite polynomials. Then the kernel turns out to be

$$\tilde{K}_{N2}(t_1, x_1; t_2, x_2) = e^{-\frac{1}{2}(x_1^2+x_2^2)} \sum_{n=0}^{N-1} \frac{H_n(x_1)H_n(x_2)}{\sqrt{\pi}2^n n!} e^{-(n+1/2)(t_2-t_1)}. \quad (4.36)$$

Using the integral formulas for the Hermite polynomial [25], we can rewrite this in a double integral form,

$$\tilde{K}_{N2}(t_1, x_1; t_2, x_2) = e^{-\frac{1}{2}(x^2-y^2)} \frac{\sqrt{2}e^{(N+\frac{1}{2})(t_1-t_2)}}{(2\pi i)^2} \int_{\gamma} dz_1 \int_{\Gamma} dz_2 \frac{z_1^N}{z_2^N} \frac{e^{-\frac{z_1^2}{2} + \sqrt{2}x_1 z_1 + \frac{z_2^2}{2} - \sqrt{2}x_2 z_2}}{z_1 e^{t_1-t_2} - z_2} \quad (4.37)$$

where  $\Gamma$  is a contour enclosing the origin anticlockwise and  $\gamma$  is an any path from  $-i\infty$  to  $i\infty$ . This representation of the kernel has a form suitable for the saddle point method. Performing the asymptotic analysis, one gets with  $t_j = \frac{\tau_j}{N^{1/3}}$

$$\lim_{N \rightarrow \infty} \mathbb{P}_{N2} \left[ \left( x_1^{t_j} - \sqrt{2N} \right) \sqrt{2}N^{1/6} \leq s_j \ (j = 1, 2) \right] = \det(1 + \mathcal{K}_2 \mathcal{G}). \quad (4.38)$$

Here  $\mathcal{G}(\tau_j; x) = -\chi_{(s_j, \infty)}(x)$  ( $j = 1, 2$ ) and the kernel is

$$\mathcal{K}_2(\tau_1, \xi_1; \tau_2, \xi_2) = \tilde{\mathcal{K}}_2(\tau_1, \xi_1; \tau_2, \xi_2) - \Phi_2(\tau_1, \xi_1; \tau_2, \xi_2) \quad (4.39)$$

where

$$\tilde{\mathcal{K}}_2(\tau_1, \xi_1; \tau_2, \xi_2) = \int_0^{\infty} d\lambda e^{-\lambda(\tau_1-\tau_2)} \text{Ai}(\xi_1 + \lambda) \text{Ai}(\xi_2 + \lambda), \quad (4.40)$$

$$\Phi_2(\tau_1, \xi_1; \tau_2, \xi_2) = \begin{cases} \int_{-\infty}^{\infty} d\lambda e^{-\lambda(\tau_1-\tau_2)} \text{Ai}(\xi_1 + \lambda) \text{Ai}(\xi_2 + \lambda), & \tau_1 < \tau_2, \\ 0, & \tau_1 \geq \tau_2. \end{cases} \quad (4.41)$$

This is a generalization of (4.22). This describes the stochastic dynamics of the largest eigenvalue of the tGUE in the scaling limit and is called the Airy process [12, 30].

The weight (4.27) is for the stationary situation. One can also consider the case where the dynamics is still  $\beta = 2$  but the initial condition is taken to be GOE or GSE. This describes the transition from the GOE or GSE to the GUE. For these transition ensembles, a similar analysis as above is possible [31]. For the dynamics of the GOE( $\beta = 1$ ) and GSE( $\beta = 4$ ) cases, however, much less is known as already mentioned.

## 5 Discrete polynuclear growth model

In section 3, we have obtained a formula for the current fluctuation by mapping the problem to that of combinatorics of Young tableaux. In this section we derive a generalized result by introducing the discrete polynuclear growth (dPNG) model [30].

The dPNG model can be defined by interpreting  $G(i, j)$  as a height of a surface. Let us introduce a new coordinate (Fig. 5),

$$s = i + j - 1, \quad x = i - j \quad (5.1)$$

and set  $h^x(s) = G(i, j)$ . In the dPNG model  $s$  and  $x$  play the role of time and space respectively and  $h^x(s)$  is considered as the height of a surface at time  $s$  and at position  $x$ . From the definition of  $G(M, N)$  (3.2), the growth dynamics of  $h^x(s)$  is given by

$$h^x(s+1) = \max\{h^{x-1}(s), h^{x+1}(s)\} + w_{\frac{s+x}{2}+1, \frac{s-x}{2}+1}. \quad (5.2)$$

Here  $w_{i,j}$  is the waiting time matrix  $w = \{w_{i,j}\}$  and is taken to be zero if  $(s+x)/2+1$  or  $(s-x)/2+1$  is not an integer. The time evolution of  $h^x(s)$  until just before  $s=3$  for our example is depicted in Fig. 6.

The above definition can be restated as follows. At time  $s=0$ , the surface is flat;  $h^x(0) = 0$  for all  $x$ . At each time  $s$ , nucleations occur at sites  $x = -s+1, -s+3, \dots, s-3, s-1$ . A nucleation at each site is independent and the height of a nucleation at each site obeys the geometric distribution with parameter  $q$ . In the meantime the surface also grows laterally in both directions deterministically with unit speed. Sometimes two steps collide whence the height is taken to be the higher one. The dPNG model is a model of stochastically growing surface.

We further introduce the multi-layer version of the dPNG model as follows. Suppose that there are infinitely many layers below the original surface. We denote the height of the  $j$ th layer by  $h_j^x(s)$  ( $j = 1, 2, \dots$ ). In particular  $h_1^x(s) = h^x(s)$ . Initially they are equally spaced as  $h_j^x(0) = 1 - j$ . The growth of the  $j$ th ( $j \geq 2$ ) layer is determined by the layer above. When there occurs a collision with height  $l$  at  $(j-1)$ th layer, then there occurs a nucleation with height  $l$  at the same position of the  $j$ th layer. They also grows laterally in both directions with unit speed but there are no stochastic nucleations. This is the multi-layer PNG model. A snapshot of a Monte-Carlo simulation is shown in Fig. 7.

For a given time  $s$  if we regard the PNG space coordinate  $x$  as time and the height coordinate  $h$  as space, the multilayers can be considered as a system of random walkers with the non-colliding condition. This kind of object has been known as vicious walks in statistical physics [32]. The weight of the non-colliding walkers (or, line ensembles) is known to be simply given by a product of determinants with entries being transition weight of each walker. Mathematically this follows from the Lindström-Gessel-Viennot theorem [33, 34]. Since our main interest is to study  $N(t)$  and  $h^0(2N-1) = G(N, N)$ , let us fix  $s = 2N - 1$  and write  $h_j^x = h_j^x(2N - 1)$  in the sequel. The transition weight of each walker at each time step is given by

$$\phi_{x,x+1}^{\text{dP}}(h_1, h_2) = \begin{cases} (1 - \sqrt{q})q^{(h_2-h_1)/2}, & h_2 \geq h_1, \\ 0, & h_2 < h_1, \end{cases} \quad (5.3)$$

when  $x$  is odd and

$$\phi_{x,x+1}^{\text{dP}}(h_1, h_2) = \begin{cases} 0, & h_2 > h_1, \\ (1 - \sqrt{q})q^{(h_1-h_2)/2}, & h_2 \leq h_1, \end{cases} \quad (5.4)$$

when  $x$  is even. This is a consequence of the fact that a nucleation of a height  $l$  occurs with probability proportional to  $q^l$ . The transition weight from  $x_1$  to  $x_2$  is given by the convolution from  $\phi_{x_1, x_1+1}$  through  $\phi_{x_2-1, x_2}$  and is compactly given by an integral formula,

$$\phi_{x_1, x_2}^{\text{dP}}(h_1, h_2) = \begin{cases} \frac{(1-\sqrt{q})^{x_2-x_1}}{2\pi i} \int_{C_1} dz z^{h_2-h_1-1} (1-\sqrt{q}z_1)^{(x_1-x_2)/2} (1-\sqrt{q}/z_1)^{(x_1-x_2)/2}, & x_1 < x_2, \\ 0, & x_1 \geq x_2, \end{cases} \quad (5.5)$$

where  $C_R$  is the contour enclosing the origin anticlockwise with radius  $R$ . The weight of the vicious walks that their positions are  $\{h_j^x\}$  is simply given by a product of determinants of this transition weight,

$$\prod_{x=-2N+1}^{2N-2} \det(\phi_{x, x+1}^{\text{dP}}(h_j^x, h_l^{x+1})) \quad (5.6)$$

with the initial and final condition  $h_j^{-2N+1} = h_j^{2N-1} = 1-j$  ( $j = 1, 2, \dots$ ). Since the number of layers is infinite, the determinant on RHS is in principle infinite dimensional. But it can be regularized by restricting the number of layers to be finite for a moment and then taking the limit.

Notice a similarity of this weight (5.6) to the joint density of tGUE (4.27). One can use a similar argument to express the joint distribution of the top layer in the form of the Fredholm determinant. It reads

$$\mathbb{P}[h_1^{x_1} \leq u_1, h_1^{x_2} \leq u_2] = \det(1 + K_N^{\text{dP}} g) \quad (5.7)$$

where the kernel is (for even  $x_1, x_2$ )

$$K_N^{\text{dP}}(x_1, h_1; x_2, h_2) = \tilde{K}_N^{\text{dP}}(x_1, h_1; x_2, h_2) - \phi_{x_1, x_2}^{\text{dP}}(h_1, h_2) \quad (5.8)$$

with

$$\tilde{K}_N^{\text{dP}}(x_1, h_1; x_2, h_2) = \sum_{j, l=1}^{\infty} \psi_j^{(x_1)}(h_1) [A^{-1}]_{j, l} \varphi_l^{(x_2)}(h_2). \quad (5.9)$$

Here

$$A_{j, l} = \phi_{-2N+1, 2N-1}^{\text{dP}}(1-j, 1-l), \quad (5.10)$$

$$\varphi_{j-1}^{(x)}(h) = \phi_{-2N+1, x}^{\text{dP}}(1-j, h), \quad (5.11)$$

$$\psi_{j-1}^{(x)}(h) = \phi_{x, 2N-1}^{\text{dP}}(h, 1-j), \quad (5.12)$$

for  $j, l = 1, 2, \dots$ . The next step is the computation of the inverse matrix  $A^{-1}$ . For the present case, it can be obtained by utilizing the fact that  $A$  is a Toeplitz matrix, leading to the kernel [18],

$$\tilde{K}_N^{\text{dP}}(x_1, h_1; x_2, h_2) = \frac{(1-\sqrt{q})^{x_2-x_1}}{(2\pi i)^2} \int_{C_{R_1}} \frac{dz_1}{z_1^{h_1}} \int_{C_{R_2}} dz_2 \frac{z_2^{h_2-1}}{z_1 - z_2} \frac{(1-\sqrt{q}/z_1)^{N+x_1/2} (1-\sqrt{q}z_2)^{N-x_2/2}}{(1-\sqrt{q}z_1)^{N-x_1/2} (1-\sqrt{q}/z_2)^{N+x_2/2}}, \quad (5.13)$$

where  $\sqrt{q} < R_2 < R_1 < 1/\sqrt{q}$  [30]. This is similar to the kernel for the tGUE (4.37).

Our original interest was to consider  $h^0(2N - 1)$  which is directly related to  $N(t)$ . But in the surface growth picture it is natural to extend our analysis to the equal-time (in  $s$ ) multi-point distribution because it is related to the roughness of the surface. One can show that the scaled height

$$\frac{h^x(s = 2N - 1) - a(b_0 + \frac{c(b_0)\tau}{N^{1/3}})N}{d(b_0)N^{1/3}} \quad (5.14)$$

with  $x = 2b_0N + 2c(b_0)N^{2/3}\tau$  tends to the Airy process as  $N \rightarrow \infty$  where

$$a(b) = \frac{2\sqrt{q}}{1-q} \left( \sqrt{q} + \sqrt{1-b^2} \right), \quad (5.15)$$

$$d(b) = \frac{q^{\frac{1}{6}}}{(1-q)(1-b^2)^{\frac{1}{6}}} (\sqrt{1+b} + \sqrt{q}\sqrt{1-b})^{\frac{2}{3}} (\sqrt{1-b} + \sqrt{q}\sqrt{1+b})^{\frac{2}{3}}, \quad (5.16)$$

$$c(b) = q^{-\frac{1}{6}}(1-b^2)^{\frac{2}{3}} (\sqrt{1+b} + \sqrt{q}\sqrt{1-b})^{\frac{1}{3}} (\sqrt{1-b} + \sqrt{q}\sqrt{1+b})^{\frac{1}{3}}. \quad (5.17)$$

For  $b_0 = 0$  this was proved in [30]; the general  $b$  case is obtained as a special case of the results in [35]. Also notice that if we take  $x = 0$  and consider the fluctuation at the origin, this reduces to (3.9). It is possible to translate this result into the language of the TASEP by noticing that  $h^x(s)$  corresponds to the time at which the  $\frac{s-x+1}{2}$ th particle has made the  $\frac{s+x+1}{2}$ th hop. It gives a joint distribution of the times at which ASEP particles pass certain bonds. It should be remarked here that the equal-time in PNG picture does not correspond to the equal-time in TASEP.

In our argument the multi-layers were introduced as an auxiliary object which makes it possible to analyze the properties of the original surface related to the quantities in TASEP. From the random matrix point of view, the multi-layers have a meaning that in the limit the behaviors of the  $j$ th layer is the same as the  $j$ th largest eigenvalue of GUE. Moreover if we set

$$h_j^x = \lambda_j^x - j + 1 \quad (j = 1, 2, \dots), \quad (5.18)$$

the probability distribution of  $\{\lambda_j^x\}$  is known to be a special case of the Schur process [36,37] which assigns the weight of the form,

$$s_{\lambda^{(1)}}(\rho_0^+) s_{\lambda^{(1)}/\mu^{(1)}}(\rho_1^-) s_{\lambda^{(2)}/\mu^{(1)}}(\rho_1^+) \cdots s_{\lambda^{(N)}/\mu^{(N-1)}}(\rho_{N-1}^+) s_{\lambda^{(N)}}(\rho_N^-), \quad (5.19)$$

on the set of Young diagrams satisfying

$$\lambda^{(1)} \supset \mu^{(1)} \subset \lambda^{(2)} \supset \mu^{(2)} \cdots \supset \mu^{(N-1)} \subset \lambda^{(N)}. \quad (5.20)$$

Here  $s_{\rho/\mu}(\rho)$  is the Schur function with the specialization of algebra  $\rho$ . In particular for  $x = 0$ , the probability distribution of  $\lambda = \{\lambda_j^0\}_{j=1,2,\dots}$  is proportional to

$$s_{\lambda(\underbrace{\sqrt{q}, \dots, \sqrt{q}}_N, 0, \dots)}^2. \quad (5.21)$$

Restriction of our attention only to  $\lambda_1$  gives another derivation of (3.6).

The limiting case of cTASEP has been studied in detail in [38, 39].

In the PNG picture, there is another limit of much interest:  $q \rightarrow 0, N \rightarrow \infty$  with  $\sqrt{q}N$  fixed. This corresponds to the continuous PNG model in which time  $s$  and space  $x$  coordinate are continuous and the height  $h$  takes integer values. In the study of the 1D KPZ systems using random matrix techniques, this model has been studied most extensively [11, 12, 40–42]. From the universality there is little doubt that the continuous PNG model and the TASEP give the same results for the quantities which are not model dependent and characteristic of the KPZ universality class.

## 6 Variants

So far we have concentrated on the current fluctuation for the step initial condition. It is also possible to generalize the analysis to some other initial conditions, boundary conditions and quantities.

### 6.1 External sources

One can generalize initial conditions to the  $\rho_-, \rho_+$  situation in which the sites on the negative side are occupied with the stationary measure with density  $\rho_-$  and the sites on the positive side with the one with density  $\rho_+$ . Of course  $\rho_- = 1, \rho_+ = 0$  corresponds to the step initial condition. In the stationary measure with density  $\rho$  the waiting time of each particle is geometrically distributed with parameter  $1 - J(\rho)/\rho$ . In the language of  $G(i, j)$  this situation can be realized by setting  $G(1, j)$  (resp.  $G(i, 1)$ ) as a geometric random variable with parameter  $1 - J(\rho_-)/\rho_-$  (resp.  $1 - J(\rho_+)/\rho_+$ ). This interpretation is explained in more detail for the cTASEP case in [41]. In the dPNG model this corresponds to the model with external sources. The fluctuation of the height at the origin was studied in [43] and those at multi-points in [44]. They are readily translated into the language of the ASEP.

### 6.2 Stationary Two point function

One of the most important achievements in the application of the methods of random matrix theory is that the stationary two point function for the 1D KPZ universality class has been computed quite explicitly by Ferrari, Prähofer and Spohn. In the PNG picture this is related to the limiting case of  $\rho_- = \rho_+$  for the model with external sources above. We do not go into details here. See the references [39, 41, 42].

### 6.3 Alternating initial condition.

Another tractable initial condition is the alternating initial condition in which initially all even sites are occupied and all odd sites are empty (Fig. 8). In the dPNG picture the surface

is initially flat. The nucleations occur at all even sites at even time and at all odd sites at odd time. This should be contrasted to the step case in which the nucleations at time  $s$  occur only at sites  $|x| < s$ . In addition although the alternating case macroscopically looks the same as for the stationary case with density  $\rho = 1/2$ , it turns out that the fluctuation is different.

The fluctuation of  $G(N, N)$  can be studied by using a symmetry property of the combinatorial approach and is shown to be  $F_1(s)$  which appeared in (4.25) as the largest eigenvalue distribution of the GOE [45, 46]. It is also possible to define the multi-layer PNG model. From the symmetry, the weight of  $\lambda$  defined from the height of multilayers by (5.18) is given by

$$s_\lambda(\underbrace{\sqrt{q}, \dots, \sqrt{q}}_N, 0, \dots) \quad (6.1)$$

where partition  $\lambda$  is restricted to ones such that it has the form  $\lambda = 2\mu$  where  $\mu$  is another partition. From this one can show that the fluctuations of the multi-layers at the origin are the same as the largest eigenvalues of GOE. Combined with the fact that the flat case is statistically translationally invariant, this suggests that the multi-layers are the same as the GOE Dyson's Brownian motion (tGOE) as conjectured in [47]. But unfortunately the analysis of the multi-layers for the flat case has been difficult. For the multi point joint distribution, at least for now, we need to employ a little different method which will be explained in subsection 7.4.

## 6.4 Half-infinite system

In the study of the ASEP, the boundary effects are important. The random matrix techniques also allow to study some properties of the half-infinite system in which the particle can enter the system at the origin with probability  $\gamma\sqrt{q}$  ( $0 < \gamma < 1/\sqrt{q}$ ) if the site is empty. In the language of  $G(i, j)$  this can be realized by putting the symmetry condition  $G(i, j) = G(j, i)$ . The symmetrized version of combinatorial approach was studied in [45, 46]. As the fluctuation of  $G(N, N)$  there appear  $F_1(s)$  and  $F_4(s)$  in (4.25) depending on the value of  $\gamma$ . In the ASEP language this says that the fluctuation of the current at the origin, i.e., the number of particles which entered the system in time  $t$  is equivalent to that of the largest eigenvalue of the GOE and GSE in the scaling limit. The current at other points were studied in [48]. There the fluctuation of the current near the origin is shown to be described by the transition ensembles mentioned in section 3.

## 6.5 Position of particles

So far we have mainly studied the fluctuation of the current, i.e. the number of particles which crossed a given bond until time  $t$ . It is also interesting to consider a related quantity, the position of particles at a given time  $t$ . In this section, we consider the step initial condition.

Let us denote the position of the  $N$ th particle at time  $t$  by  $x_N(t)$ . If we remember that  $G(M, N) + M + N - 1$  is the time at which the  $N$ th particle has made the  $M$ th jump,

properties of  $x_N(t)$  for a single particle can be obtained by a translation of results for the current. If we take  $t \rightarrow \infty$  limit for a fixed  $N$ , it is known that  $x_N(t)$  goes to the dynamics of the largest eigenvalue of GUE [49]. Here we consider another limit  $t \rightarrow \infty, N \rightarrow \infty$  with  $\nu = N/t$  fixed. The quantity  $x_{\nu t}(t)/t$  has a deterministic limit,

$$\lim_{t \rightarrow \infty} (x_{\nu t}(t) + \nu t - 1)/t = a^*(\nu) \quad (6.2)$$

where

$$a^*(\nu) = \begin{cases} 1 - q - (1 - 2q)\nu - 2\sqrt{\nu(1 - \nu)q(1 - q)}, & 0 < \nu < 1, \\ 0, & \nu > 1. \end{cases} \quad (6.3)$$

For a single particle, the fluctuation of  $x_N(t)$  around this position can also be obtained from the result for the current by setting  $\tau = 0$  in (5.14).

It is further possible to study the equal time joint distribution of the position of several particles by introducing a multi-layer PNG model which is a little different from the one in section 5. See Fig. 9. It is defined as follows. Let  $k_j^v(t)$  be a height of the  $j$ th ( $j = 1, 2, \dots$ ) layer at time  $t$  ( $= 0, 1, 2, \dots$ ) and at position  $v = 0, 1, 2, \dots$ . Initially they are all flat;  $k_j^v(0) = 1 - j$  for all  $v$ . At each time  $t$  at each layer nucleations of height one may occur at sites  $v = 1, 3, \dots, 2t - 1$  with the condition that the layers do not touch. Here a nucleation at each site is independent, has a shape depicted as in Fig. 9, and occurs with probability  $q$ . In the meantime it grows laterally to the right with speed 2. Notice a similarity and difference between the PNG model here and that in section 5. This is the same as the DR-paths in the Aztec diamond [50, 51]. One can confirm oneself that the dynamics of the top layer  $k^v(t) = k_1^v(t)$  gives, if set

$$x_N(t) = t - 2N + 2 - k^{2N-1}(t), \quad (6.4)$$

the correct statistical properties of the TASEP particle positions.

The multi-layers in this PNG model can again be regarded as vicious walks. The transition weight of each walker is now

$$\phi_{v,v+1}^*(k_1, k_2) = \begin{cases} p^{k_2 - k_1}, & k_2 \geq k_1, \\ 0, & k_2 < k_1, \end{cases} \quad (6.5)$$

with  $p = q/(1 - q)$  when  $v$  is even and

$$\phi_{v,v+1}^*(k_1, k_2) = \begin{cases} 1, & k_2 = k_1, k_1 - 1, \\ 0, & \text{otherwise,} \end{cases} \quad (6.6)$$

when  $v$  is odd. The weight of the vicious walks are simply given by a product of determinant of this transition weight,

$$\prod_{v=0}^{2N-1} \det(\phi_{v,v+1}^*(k_j^v, k_l^{v+1})) \quad (6.7)$$

with the initial and final condition  $k_j^0 = k_j^{2N} = 1 - j$  ( $j = 1, 2, \dots$ ).

The joint distribution has the form,

$$\begin{aligned} & \mathbb{P}[x_{r_1}(t) \geq t - 2r_1 + 2 - u_1, x_{r_2}(t) \geq t - 2r_2 + 2 - u_2] \\ &= \mathbb{P}[k^{2r_1-1}(t) \leq u_1, k^{2r_2-1}(t) \leq u_2] = \det(1 + K_t^* g) \end{aligned} \quad (6.8)$$

where the kernel is given by

$$K_t^*(r_1, k_1; r_2, k_2) = \tilde{K}_t^*(r_1, k_1; r_2, k_2) - \phi_{r_1, r_2}^*(k_1, k_2), \quad (6.9)$$

with

$$K_t^*(r_1, k_1; r_2, k_2) = \frac{1}{(2\pi i)^2} \int_{C_{R_1}} \int_{C_{R_2}} dz_1 dz_2 \frac{z_1^{k_1-1}}{z_2^{k_2+1}} \frac{z_2}{z_2 - z_1} \frac{(1 + 1/z_1)^{t-r_1+1} (1 - pz_1)^{r_1}}{(1 + 1/z_2)^{t-r_2+1} (1 - pz_2)^{r_2}}, \quad (6.10)$$

$$\phi_{r_1, r_2}^*(k_1, k_2) = \frac{1}{2\pi i} \int_{C_R} dz \frac{1}{z^{k_2-k_1+1}} \left( \frac{1 + 1/z}{1 - pz} \right)^{r_2-r_1} \quad (6.11)$$

where  $R_1 < R_2$  and  $0 < R < 1$ . Applying the asymptotic analysis, one can show that

$$\frac{a^*(b)t - bt + 1 - x_N(t)}{d^*(b)t^{1/3}} \quad (6.12)$$

with  $N = \nu t + 2c^*(\nu)t^{2/3}\tau$  tends to the Airy process where

$$a^*(\nu) = (1 - q) - (1 - 2q)\nu - 2\sqrt{\nu(1 - \nu)q(1 - q)}, \quad (6.13)$$

$$d^*(\nu) = (\nu(\nu - 1))^{\frac{1}{6}} q^{\frac{1}{2}} (1 - q)^{\frac{1}{2}} \left( 1 + \sqrt{\frac{\nu(1 - q)}{q(\nu - 1)}} \right)^{\frac{2}{3}} \left( \sqrt{\frac{\nu - 1}{\nu}} - \sqrt{\frac{q}{1 - q}} \right)^{\frac{2}{3}}, \quad (6.14)$$

$$c^*(\nu) = (\nu(\nu - 1))^{\frac{5}{6}} \left( 1 + \sqrt{\frac{\nu(1 - q)}{q(\nu - 1)}} \right)^{\frac{1}{3}} \left( \sqrt{\frac{\nu - 1}{\nu}} - \sqrt{\frac{q}{1 - q}} \right)^{\frac{1}{3}}. \quad (6.15)$$

In the cTASEP limit, (6.12) with (6.15) replaced by

$$a^*(\nu) = (\sqrt{\nu} - 1)^2, \quad (6.16)$$

$$d^*(\nu) = \nu^{1/6} (\sqrt{1/\nu} - 1)^{2/3}, \quad (6.17)$$

$$c^*(\nu) = \nu^{5/6} (\sqrt{1/\nu} - 1)^{1/3} \quad (6.18)$$

tends to the Airy process.

What have been explained in this subsection is the equal-time multi-particle joint distribution. It is also possible to study the multi-time joint distribution of the position of a single particle (tagged particle) [49].

## 7 Green's function method

So far we have explained how the fluctuation is computed by combining a combinatorial argument and techniques from random matrix theory. There is a related but a somehow different method using the Green's function for the TASEP. This is the probability that the particles starting from sites  $y_1, \dots, y_N$  ( $y_1 > y_2 > \dots > y_N$ ) at time 0 are on sites  $x_1, \dots, x_N$  ( $x_1 > x_2 > \dots > x_N$ ) at time  $t$  and is also called the transition probability. We denote this quantity by  $G(x_1, \dots, x_N; t | y_1, \dots, y_N; 0)$  or, when we fix the initial condition, by  $G(x_1, \dots, x_N; t)$ . For the cTASEP, a determinantal formula was obtained by Schütz [52]. In this section we explain some applications of the formula. In this section we only consider the continuous time case. For the discrete case the expression for the Green's function was obtained in [53] but has not been exploited to obtain the results in the scaling limit. See also [54].

### 7.1 Formula

First let us remember the formula [52]. It reads

$$G(x_1, x_2, \dots, x_N; t) = \det[F_{l-j}(x_{N-l+1} - y_{N-j+1}; t)]_{j,l=1, \dots, N} \quad (7.1)$$

where the function  $F_n(x, t)$  appearing as matrix elements of the determinant is explicitly given by

$$F_n(x; t) = e^{-t} \frac{t^x}{x!} \sum_{k=0}^{\infty} (-1)^k \frac{(n)_k}{(x+1)_k} \frac{t^k}{k!}. \quad (7.2)$$

To see the structure we write down the determinants for  $N = 1, 2$ . For  $N = 1$  this is simply

$$G(x_1; t | y_1; 0) = F_0(x - y; t) = \frac{t^{x-y}}{(x-y)!} e^{-t}. \quad (7.3)$$

For  $N = 2$  the formula gives

$$G(x_1, x_2; t) = \begin{vmatrix} F_0(x_2 - y_2; t) & F_1(x_1 - y_2; t) \\ F_{-1}(x_2 - y_1; t) & F_0(x_1 - y_1; t) \end{vmatrix}. \quad (7.4)$$

The proof of (7.1) consists of checking the master equation and the initial condition which should be satisfied by the Green's function.

Some formulas of the function  $F_n(x; t)$  which are useful in the following are given. It has an integral representation,

$$F_{-n}(x; t) = \frac{1}{2\pi i} \int_{\Gamma_{0,-1}} dw \frac{w^n}{(1+w)^{n+x+1}} e^{wt} \quad (7.5)$$

where  $\Gamma_{0,-1}$  represents a contour enclosing both  $w = 0$  and  $w = -1$  anticlockwise. They satisfy the recurrence relations,

$$\frac{d}{dt}F_n(x;t) = F_n(x-1;t) - F_n(x;t), \quad (7.6)$$

$$\int_0^t dt F_{n-1}(x-1;t) = F_n(x;t), \quad (7.7)$$

$$F_n(x;t) = \sum_{x_1=x}^{\infty} F_{n-1}(x_1;t), \quad (7.8)$$

$$F_{n-1}(x;t) = F_n(x;t) - F_n(x+1;t). \quad (7.9)$$

## 7.2 Position fluctuation of a single particle

Let us first study the fluctuation of the position of a particle. A basic observation is that the probability we are interested in is written as a sum of the Green's function,

$$\mathbb{P}[x_N(t) - y_N \geq M] = \sum_{y_N+M \leq x_N < \dots < x_1} G(x_1, \dots, x_N; t | y_1, \dots, y_N; 0). \quad (7.10)$$

Here  $\mathbb{P}$  indicates the measure of the TASEP for our current initial condition and the summation on RHS is over all  $x_i$ 's which satisfy the constraint  $y_N + M \leq x_N < \dots < x_1$ . The next thing to do is to rewrite the RHS to a form which is suitable for an asymptotic analysis. In [55,56], it was shown that the quantity can be written in the form of a multiple integral which reduces to (3.11) for the step initial condition.

In this subsection we state a similar result for the fluctuation of  $x_N(t)$  for the step initial condition, i.e., for  $y_j = 1 - j$  ( $j = 1, \dots, N$ ). We have

$$\mathbb{P}[x_N(t) + N - 1 \geq M] = \frac{1}{Z} \sum_{x_1=M}^{\infty} \dots \sum_{x_N=M}^{\infty} \prod_{1 \leq j < l \leq N} (x_j - x_l)^2 \prod_{j=1}^N \frac{t^{x_j} e^{-t}}{x_j!} \quad (7.11)$$

with

$$Z = t^{N(N-1)/2} \prod_{j=1}^N j!. \quad (7.12)$$

Since the orthogonal polynomials for the weight  $\frac{t^x e^{-t}}{x!}$  is called the Charlier orthogonal polynomials [27], this expression could be called the Charlier ensemble representation of the fluctuation of  $x_N(t)$ . The proof is almost the same as in [55] and is omitted here. But to illustrate the method we give a step-by-step calculation for the  $N = 2$  case. It proceeds

as follows.

$$\begin{aligned}
\mathbb{P}[x_2(t) \geq M-1] &= \sum_{M-1 \leq x_2 < x_1} G(x_1, x_2; t | 0, -1; 0) \\
&= \sum_{M-1 \leq x_2 < x_1} \begin{vmatrix} F_0(x_2+1; t) & F_1(x_1+1; t) \\ F_{-1}(x_2; t) & F_0(x_1; t) \end{vmatrix} \\
&= \sum_{M-1 \leq x_2 < x_1} \sum_{y_1=x_1}^{\infty} \begin{vmatrix} F_0(x_2+1; t) & F_0(y_1+1; t) \\ F_{-1}(x_2; t) & F_{-1}(y_1; t) \end{vmatrix}. \tag{7.13}
\end{aligned}$$

If we denote the determinant on the RHS by  $f(x_2, y_1)$ , this is equal to

$$\begin{aligned}
\sum_{x_2=M-1}^{\infty} \sum_{x_1=x_2+1}^{\infty} \sum_{y_1=x_1}^{\infty} f(x_2, y_1) &= \sum_{x_2=M-1}^{\infty} \sum_{y_1=x_2+1}^{\infty} \sum_{x_1=x_2+1}^{y_1} f(x_2, y_1) \\
&= \sum_{x_2=M}^{\infty} \sum_{y_1=x_2+1}^{\infty} (y_1 - x_2) f(x_2, y_1) = \sum_{x_2=M}^{\infty} \sum_{x_1=x_2+1}^{\infty} (x_1 - x_2) f(x_2, x_1). \tag{7.14}
\end{aligned}$$

Since

$$\begin{aligned}
f(x_2, x_1) &= \begin{vmatrix} F_0(x_2+1; t) & F_0(x_1+1; t) \\ F_0(x_2; t) - F_0(x_2+1; t) & F_0(x_1; t) - F_0(x_1+1; t) \end{vmatrix} \\
&= \begin{vmatrix} \frac{t^{x_2+1}}{(x_2+1)!} e^{-t} & \frac{t^{x_1+1}}{(x_1+1)!} e^{-t} \\ \frac{t^{x_2}}{x_2!} e^{-t} & \frac{t^{x_1}}{x_1!} e^{-t} \end{vmatrix} = \frac{t^{x_1+x_2+1} e^{-2t}}{(x_1+1)!(x_2+1)!} (x_1 - x_2), \tag{7.15}
\end{aligned}$$

we have

$$\begin{aligned}
\mathbb{P}[x_2(t) \geq M-1] &= \sum_{x_2=M+1}^{\infty} \sum_{x_1=x_2+1}^{\infty} (x_2 - x_1)^2 \frac{t^{x_1+x_2+1}}{(x_1+1)!(x_2+1)!} e^{-2t} \\
&= \frac{1}{2t} \sum_{x_1=M}^{\infty} \sum_{x_2=M}^{\infty} (x_2 - x_1)^2 \frac{t^{x_1+x_2}}{x_1!x_2!} e^{-2t}. \tag{7.16}
\end{aligned}$$

This is nothing but the expression (7.11), (7.12) for  $N = 2$ .

### 7.3 Position of particles: Step case

In the previous subsection we considered the fluctuation of a single particle. To study the joint distribution, the original form of the Green's function is not very convenient. We rewrite it in a form such that the position of particles can be regarded as a dynamics of the first walker in a certain vicious walk [57, 58].

Let us consider a determinantal weight,

$$\prod_{r=1}^{N-1} \det[\phi_{r,r+1}^G(x_j^r, x_l^{r+1})]_{j,l=1,\dots,r+1} \cdot \det[\psi_j^{(N)}(x_l^N)]_{j=0,\dots,N-1, l=1,\dots,N} \tag{7.17}$$

under the condition  $x_1^2 < x_2^2, x_1^3 < x_2^3 < x_3^3, \dots$  and the convention  $\phi_{r,r+1}^G(x_{r+1}^r; x_j^{r+1}) = 1$  for  $r = 1, \dots, N-1, j = 1, \dots, r+1$ . Here the functions  $\psi_j^{(r)}(x)$  and  $\phi_{r_1, r_2}^G(x, y)$  are defined by

$$\psi_j^{(r)}(x) = (-1)^{r-1-j} F_{-r+1+j}(x - y_{j+1}, t) = \frac{(-1)^{r-1-j}}{2\pi i} \int_{\Gamma_{0,-1}} dw \frac{w^{r-1-j}}{(1+w)^{x+r-j-y_{j+1}}} e^{wt} \quad (7.18)$$

and

$$\phi_{r_1, r_2}^G(x_1, x_2) = \begin{bmatrix} x_1 - x_2 - 1 \\ r_2 - r_1 - 1 \end{bmatrix}. \quad (7.19)$$

In particular

$$\phi_{r, r+1}^G(x_1, x_2) = \begin{cases} 1, & x_1 > x_2, \\ 0, & x_1 \leq x_2. \end{cases} \quad (7.20)$$

This can be considered as a weight of a vicious walk (Fig. 10). A different feature from (5.6) and (6.7) is that the number of particles is not fixed in (7.17).

Let  $\mathbb{P}_G$  denote the corresponding measure. Then we have

$$G(x_1, \dots, x_N; t) = \mathbb{P}_G[x_1^1 = x_1, x_1^2 = x_2, \dots, x_1^N = x_N]. \quad (7.21)$$

For  $N = 2$  this reads

$$\begin{aligned} G(x_1, x_2; t) &= \begin{vmatrix} F_0(x_2 - y_2; t) & F_1(x_1 - y_2; t) \\ F_{-1}(x_2 - y_1; t) & F_0(x_1 - y_1; t) \end{vmatrix} \\ &= \sum_{x_2^{(2)}(>x_1^2)} \begin{vmatrix} \phi_{1,2}^G(x_1^1, x_1^2) & \phi_{1,2}^G(x_1^1, x_2^2) \\ 1 & 1 \end{vmatrix} \begin{vmatrix} \psi_0^{(2)}(x_1^2) & \psi_0^{(2)}(x_2^2) \\ \psi_1^{(2)}(x_1^2) & \psi_1^{(2)}(x_2^2) \end{vmatrix} \end{aligned}$$

where  $x_1^1 = x_1, x_1^2 = x_2$  and can be proved easily by using properties the determinant and  $F_n(x; t)$ . The proof for general  $N$  is similar and is given in [58]. The merit of rewriting this way is that the weight (7.17) has a similar form to (4.27) for tGUE. As a consequence we can describe the joint distribution by a Fredholm determinant. The kernel takes the form,

$$K_{N2}^G(r_1, x_1; r_2, x_2) = \tilde{K}_{N2}^G(r_1, x_1; r_2, x_2) - \phi_{r_1, r_2}^G(x_1, x_2) \quad (7.22)$$

with

$$\tilde{K}_{N2}^G(r_1, x_1; r_2, x_2) = \sum_{j=0}^{N-1} \psi_j^{(r_1)}(x_1) \varphi_j^{(r_2)}(x_2) \quad (7.23)$$

where  $\varphi_j^{(r)}$  is a polynomial orthonormal to  $\psi_j^{(r)}$ . For the step initial condition for which  $y_{j+1} = -j, \varphi_j^{(r)}$  ( $j = 0, 1, \dots, N-1$ ) can be taken as

$$\varphi_j^{(r)}(x) = \frac{(-1)^{r-1-j}}{2\pi i} \int_{\Gamma_0} dz \frac{(1+z)^{x+r-1}}{z^{r-j}} e^{-zt}, \quad (7.24)$$

where  $\Gamma_0$  is the contour enclosing the origin anticlockwise. As a result we have a double integral expression of the kernel,

$$\begin{aligned} K_{N2}^G(r_1, x_1; r_2, x_2) &= \tilde{K}_{N2}^G(r_1, x_1; r_2, x_2) - \phi_{r_1, r_2}^G(x_1, x_2), \\ \tilde{K}_{N2}^G(r_1, x_1; r_2, x_2) &= \int_{\Gamma_{-1}} \frac{dw}{2\pi i} \int_{\Gamma_0} \frac{dz}{2\pi i} \frac{(1+z)^{x_2+r_2-1} (-w)^{r_1} e^{(w-z)t}}{(1+w)^{x_1+r_1} (-z)^{r_2} (w-z)}. \end{aligned} \quad (7.25)$$

By doing the asymptotic analysis as usual, we can reproduce the result in subsection 6.5 for the cTASEP.

## 7.4 Position of particles: Alternating case

In the previous two subsections we have seen that the method using the Green's function allows us to reproduce the results for the step initial condition, which were obtained by a combinatorial approach. A big advantage of the method of using the Green's function is that one can deal with arbitrary initial configuration of particles at least up to some stage of the analysis.

In particular in [57, 58] the joint distribution for the alternating case was analyzed. For a technical reason we take the initial condition to be  $y_{j+1} = -2j$  ( $j = 0, 1, \dots, N-1$ ). But if we take  $t$  finite and  $N$  large enough, deep inside the negative region  $x(\leq 0)$  the dynamics of particles is the same as that for the alternating initial condition. Remember here that up to now the multi-layer PNG techniques have not been successfully applied to obtain the multi-point statistics for this initial condition. The discussions are the same as for the step case until (7.23). The difference is that this time we employ a different set of  $\varphi_j^{(r)}$ 's which are orthonormal to  $\psi_j^{(r)}$ 's. The functions are found to be

$$\varphi_j^{(r)}(x) = \frac{(-1)^{r-1-j}}{2\pi i} \int_{\Gamma_0} dz \frac{1+2z}{1+z} \frac{(1+z)^{x+r+j-1}}{z^{r-j}} e^{-zt}. \quad (7.26)$$

Then the kernel becomes

$$\begin{aligned} K_{N1}^G(r_1, x_1; r_2, x_2) &= \tilde{K}_{N1}^G(r_1, x_1; r_2, x_2) - \phi_{r_1, r_2}^G(x_1, x_2), \\ \tilde{K}_{N1}^G(r_1, x_1; r_2, x_2) &= \int_{\Gamma_{-1}} \frac{dw}{2\pi i} \int_{\Gamma_0} \frac{dz}{2\pi i} \frac{(1+z)^{x_2+r_2-2} (-w)^{r_1} (1+2z) e^{(w-z)t}}{(1+w)^{x_1+r_1-1} (-z)^{r_2} (w-z)(1+w+z)}. \end{aligned} \quad (7.27)$$

By applying the saddle point analysis, one gets a limiting kernel which is different from (4.39). Though (7.27) looks similar to (7.25), the pole at  $z = -1 - w$  makes the situation completely different.

## 8 Concluding Remarks

In this paper we have discussed the applications of random matrix techniques to the study of fluctuations of the one-dimensional totally asymmetric simple exclusion process (TASEP).

Besides a brief review of the techniques, we have explained three approaches. The first one is the combinatorial approach, the second is the discrete polynuclear growth model and the last one is the Green's function method. The point is that in all these approaches there appear some objects whose weight can be described by a product of determinants and that the same kind of weight appears in the random matrix theory. We have mainly explained the methods and results for the step initial condition. Other cases including the alternating initial condition are also briefly explained. We have also seen the relationship of the TASEP to the directed polymer in random medium and the two types of the polynuclear growth models.

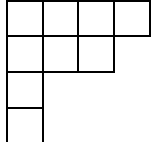
In spite of its many successful applications, it has not yet been clear to what extent this method could be extended to study other properties of the ASEP. In fact there are a lot of open questions. For instance the correlation of the current at the origin  $N(t_1), N(t_2)$  at two times is a natural quantity to consider, but we don't know if it is handled by a generalization of the random matrix techniques at the moment. More studies with new ideas are certainly desired.

## Acknowledgment

The author would like to thank T. Tanemura, M. Katori and T. Imamura for fruitful discussions. This work is partly supported by the Grant-in-Aid for Young Scientists (B), the Ministry of Education, Culture, Sports, Science and Technology, Japan.

## Appendix A

In this appendix we explain some definitions, notations and formulas related to the Young tableaux. The partition  $\lambda = (\lambda_1, \lambda_2, \dots)$  is a collection of nonnegative integers  $\lambda_i$ 's which satisfy  $\lambda_1 \geq \lambda_2 \geq \dots$  and is conveniently represented by a Young diagram. For instance

the partition  $\lambda = (4, 3, 1, 1)$  corresponds the Young diagram . A semistandard

Young tableau (SSYT) is a Young diagram with each box filled with a nonnegative integer with the condition that they are non-decreasing in each row and are increasing in each column. We often restrict the entries of integers to fill to be from a finite set  $\{1, 2, \dots, N\}$ .

The Schur function  $s_\lambda(x_1, x_2, \dots)$  is defined by

$$s_\lambda(x_1, x_2, \dots) = \sum_{T: \text{SSYT}} x_1^{T_1} x_2^{T_2} \dots \quad (\text{A.1})$$

where  $T_i$  is the number of  $i$  in SSYT. For instance when  $\lambda = (2, 1)$ ,  $x_4 = x_5 = \dots = 0$  and we take entries from  $\{1, 2, 3\}$ , all possible SSYTs are

$$\begin{array}{|c|c|} \hline 1 & 1 \\ \hline 2 & \\ \hline \end{array}, \begin{array}{|c|c|} \hline 1 & 1 \\ \hline 3 & \\ \hline \end{array}, \begin{array}{|c|c|} \hline 1 & 2 \\ \hline 2 & \\ \hline \end{array}, \begin{array}{|c|c|} \hline 1 & 2 \\ \hline 3 & \\ \hline \end{array}, \begin{array}{|c|c|} \hline 1 & 3 \\ \hline 2 & \\ \hline \end{array}, \begin{array}{|c|c|} \hline 1 & 3 \\ \hline 3 & \\ \hline \end{array}, \begin{array}{|c|c|} \hline 2 & 2 \\ \hline 3 & \\ \hline \end{array}, \begin{array}{|c|c|} \hline 2 & 3 \\ \hline 3 & \\ \hline \end{array} \quad (\text{A.2})$$

and hence

$$s_\lambda(x_1, x_2, x_3, 0, \dots) = x_1^2 x_2 + x_1^2 x_3 + x_1 x_2^2 + x_1 x_3^2 + x_2^2 x_3 + x_2 x_3^2 + 2x_1 x_2 x_3. \quad (\text{A.3})$$

The number of the SSYT's of shape  $\lambda$  with entries from  $\{1, 2, \dots, N\}$  is given by

$$L(\lambda, N) = s_\lambda(\underbrace{1, \dots, 1}_N, 0, \dots). \quad (\text{A.4})$$

There is another representation of the Schur function,

$$s_\lambda(x_1, \dots, x_N, 0, \dots) = \frac{\det(x_j^{\lambda_i + N - i})_{1 \leq i, j \leq N}}{\det(x_j^{N - i})_{1 \leq i, j \leq N}}. \quad (\text{A.5})$$

By putting  $x_i = \alpha^{i-1}$  ( $i = 1, \dots, N$ ) and then taking the limit  $\alpha \rightarrow 1$ , one gets a formula,

$$s_\lambda(\underbrace{1, \dots, 1}_N, 0, \dots) = \prod_{1 \leq i < j \leq N} \frac{\lambda_i - \lambda_j + j - i}{j - i}. \quad (\text{A.6})$$

## References

- [1] T. M. Liggett. *Interacting Particle Systems*. Springer-Verlag, 1985.
- [2] T. M. Liggett. *Stochastic Interacting Systems: Contact, Voter, and Exclusion Processes*. Springer-Verlag, 1999.
- [3] H. Spohn. *Large Scale Dynamics of Interacting Particles*. Springer, 1991.
- [4] G. M. Schütz. Exactly solvable models for many-body systems far from equilibrium. In C. Domb and J. L. Lebowitz, editors, *Phase Transitions and Critical Phenomena 19*, 2000.
- [5] B. Derrida, M. R. Evans, V. Hakim, and V. Pasquier. Exact solution of a 1D exclusion model using a matrix formulation. *J. Phys. A*, 26:1493–1517, 1993.
- [6] M. Kardar, G. Parisi and Y. C. Zhang. Dynamic scaling of growing interfaces. *Phys. Rev. Lett.*, 56:889–892, 1986.
- [7] A.L. Barabási and H.E. Stanley. *Fractal concepts in surface growth*. Cambridge University Press, 1995.
- [8] J. Krug and H. Spohn. Kinetic roughening of growing interfaces. In C. Godrèche, editor, *Solids far from Equilibrium: Growth, Morphology and Defects*, pages 479–582, 1992.
- [9] L.-H. Gwa and H. Spohn. Six-vertex model, roughened surfaces, and an asymmetric spin Hamiltonian. *Phys. Rev. Lett.*, 68:725–728, 1992.

- [10] D. Kim. Bethe ansatz solution for crossover scaling functions of the asymmetric XXZ chain and the Kardar-Parisi-Zhang-type growth model. *Phys. Rev. E*, 52:3512–3524, 1995.
- [11] M. Prähofer and H. Spohn. Statistical self-similarity of one-dimensional growth processes. *Physica A*, 279:342–352, 2000.
- [12] M. Prähofer and H. Spohn. Scale Invariance of the PNG Droplet and the Airy Process. *J. Stat. Phys.*, 108:1071–1106, 2002.
- [13] K. Johansson. Random matrices and determinantal processes. In A. Bovier, F. Dunlop, A. van Enter, F. den Hollander, and J. Dalibard, editors, *Mathematical Statistical Physics, Session LXXXIII: Lecture Notes of the Les Houches Summer School 2005*, pages 1–56, 2006.
- [14] H. Spohn. Exact solutions for KPZ-type growth processes, random matrices, and equilibrium shapes of crystals. *Physica A*, 369:71–99, 2006.
- [15] P. Deift. Universality for mathematical and physical systems, math-ph/063038.
- [16] P. L. Ferrari and M. Prähofer. One-dimensional stochastic growth and gaussian ensembles of random matrices, in proceedings of ”inhomogeneous random systems 2005”. *Markov Processes Relat. Fields*, 12:203–234, 2006.
- [17] W. Jockush, J. Propp, P. Shor. Random domino tilings and the arctic circle theorem, preprint 1995, math.CO/9801068.
- [18] K. Johansson. Shape fluctuations and random matrices. *Comm. Math. Phys.*, 209:437–476, 2000.
- [19] R. P. Stanley. *Enumerative Combinatorics 2*. Springer, 1999.
- [20] W. Fulton. *Young Tableaux*. Cambridge, 1997.
- [21] C. A. Tracy and H. Widom. Level-spacing distributions and the Airy kernel. *Comm. Math. Phys.*, 159:151–174, 1994.
- [22] M. L. Mehta. *Random Matrices*. Elsevier, 3rd edition, 2004.
- [23] P. J. Forrester. available from the author’s homepage, <http://www.ms.unimelb.edu.au/~matpjf/matpjf.html>.
- [24] C. A. Tracy and H. Widom. Correlation functions, cluster functions, and spacing distributions for random matrices. *J. Stat. Phys.*, 92:809–835, 1998.
- [25] G. E. Andrews, R. Askey, and R. Roy. *Special Functions. volume 71 of Encyclopedia of Mathematics and its Applications*. Cambridge University Press, 1999.

- [26] G. Szegő. *Orthogonal Polynomials*. AMS, 1975.
- [27] R. Koekoek and R. F. Swarttouw. The Askey-scheme of hypergeometric orthogonal polynomials and its  $q$ -analogue, math.CA/9602214.
- [28] C. A. Tracy and H. Widom. On orthogonal and symplectic matrix ensembles. *Comm. Math. Phys.*, 177:727–754, 1996.
- [29] F. J. Dyson. A Brownian-motion model for the eigenvalues of a random matrix. *J. Math. Phys.*, 3:1191–1198, 1962.
- [30] K. Johansson. Discrete polynuclear growth and determinantal processes. *Comm. Math. Phys.*, 242:277–329, 2003.
- [31] P. J. Forrester, T. Nagao and G. Honner. Correlations for the orthogonal-unitary and symplectic transitions at the hard and soft edges. *Nucl. Phys. B*, 553:601–643, 1999.
- [32] M. E. Fisher. Walks, walls, wetting, and melting. *J. Stat. Phys.*, 34:667–729, 1984.
- [33] B. Lindström. On the vector representations of induced matroids. *Bull. London Math. Soc.*, 5:85–90, 1973.
- [34] I. Gessel and G. Viennot. Determinants, paths, and plane partitions. preprint, 1989.
- [35] T. Imamura and T. Sasamoto. Fluctuations of the one-dimensional polynuclear growth model with external sources. *Nucl. Phys. B*, 699:503–544, 2004.
- [36] A. Okounkov and N. Reshetikhin. Correlation function of Schur process with application to local geometry of a random 3-dimensional Young diagram. *J. Amer. Math. Soc.*, 16:581–603, 2003.
- [37] A. Borodin and E. M. Rains. Eynard-Mehta theorem, Schur process, and their Pfaffian analogs. *J. Stat. Phys.*, 121:291–317, 2006.
- [38] H. Spohn. KPZ equation in one dimension and line ensembles. *Pranama J. Phys.*, 64:1–11, 2005.
- [39] P. L. Ferrari and H. Spohn. Scaling limit for the space-time covariance of the stationary totally asymmetric simple exclusion process. *Comm. Math. Phys.*, 265:1–44, 2006.
- [40] M. Prähofer and H. Spohn. Universal distributions for growth processes in 1+1 dimensions and random matrices. *Phys. Rev. Lett.*, 84:4882–4885, 2000.
- [41] M. Prähofer and H. Spohn. Current fluctuations for the totally asymmetric simple exclusion process. In V. Sidoravicius, editor, *In and out of equilibrium, vol. 51 of Progress in Probability*, pages 185–204, 2002.

- [42] M. Prähofer and H. Spohn. Exact scaling functions for one-dimensional stationary KPZ growth. *J. Stat. Phys.*, 115:255–279, 2004.
- [43] J. Baik and E. M. Rains. Limiting distributions for a polynuclear growth model with external sources. *J. Stat. Phys.*, 100:523–541, 2000.
- [44] T. Imamura and T. Sasamoto. Polynuclear growth model with external source and random matrix model with deterministic source. *Phys. Rev. E*, 71:014696, 2005.
- [45] J. Baik and E. M. Rains. The asymptotics of monotone subsequences of involutions. *Duke Math. J.*, 109:205–281, 2001.
- [46] J. Baik and E. M. Rains. Symmetrized random permutations. In P. M. Bleher and A. R. Its, editors, *Random Matrix Models and Their Applications*, pages 1–29, 2001.
- [47] P. L. Ferrari. Polynuclear growth on a flat substrate and edge scaling of GOE eigenvalues. *Comm. Math. Phys.*, 252:77–109, 2004.
- [48] T. Sasamoto and T. Imamura. Fluctuations of the one-dimensional polynuclear growth model in half-space. *J. Stat. Phys.*, 115:749–803, 2004.
- [49] T. Imamura and T. Sasamoto. Dynamical properties of a tagged particle in the totally asymmetric simple exclusion process with the step-type initial condition, math-ph/0702009.
- [50] K. Johansson. Non-intersecting paths, random tilings and random matrices. *Probab. Theory Relat. Fields*, 123:225–280, 2002.
- [51] K. Johansson. The arctic circle boundary and the Airy process. *Ann. Prob.*, 33:1–30, 2005.
- [52] G. M. Schütz. Exact solution of the master equation for the asymmetric exclusion process. *J. Stat. Phys.*, 88:427–445, 1997.
- [53] A. M. Povolotsky and V. B. Priezzhev. Determinant solution for the totally asymmetric exclusion process with parallel update, cond-mat/0605150.
- [54] A. Borodin, P. L. Ferrari and M. Prähofer. Fluctuations in the discrete TASEP with periodic initial configurations and the  $\text{Airy}_1$  process, math-ph/0611071.
- [55] T. Nagao and T. Sasamoto. Asymmetric simple exclusion process and modified random matrix ensembles. *Nucl. Phys. B*, 699:487–502, 2004.
- [56] A. Rákos and G. M. Schütz. Current distribution and random matrix ensembles for an integrable asymmetric fragmentation process. *J. Stat. Phys.*, 118:511–530, 2005.
- [57] T. Sasamoto. Spatial correlations of the 1D KPZ surface on a flat substrate. *J. Phys. A*, 38:L549–L556, 2005.

- [58] A. Borodin, P. L. Ferrari, M. Prähofer, and T. Sasamoto. Fluctuation properties of the TASEP with periodic initial configuration, math-ph/0608056.

## Figure Captions

Fig. 1: The one-dimensional asymmetric simple exclusion process with parallel update.

Fig. 2: The step initial condition for the TASEP.

Fig. 3: An example of space-time trajectories of particles. The trajectories of the rightmost four particles are shown until each particle has made the fourth hops.

Fig. 4: The dynamics of the eigenvalues of the GUE Dyson's Brownian motion (tGUE).

Fig. 5: The waiting time table. The time coordinate  $s$  and space coordinate  $x$  in the discrete PNG model are also shown.

Fig. 6: The discrete PNG model. The second layer in the multi-layer PNG model is also shown. Initially at time  $s = 0$  the surface is flat and nothing happens until  $s = 1$ . At time  $s = 1$  a nucleation of height one occurs at the origin. Between time  $s = 1$  and  $s = 2$  the surface grows laterally in both directions with unit speed. The height at the origin at  $s = 3^-$  is determined by the "higher one wins" rule. The height difference 1 becomes the height of a nucleation at the second layer.

Fig. 7: A snapshot of a simulation of the multi-layer discrete PNG model. Note a similarity to the Fig. 4.

Fig. 8: The alternating initial condition for the TASEP.

Fig. 9: Another discrete PNG model in subsection 6.5. The height of the top layer gives the positions of particles through (6.4). Nucleations at a lower layer occur stochastically.

Fig. 10: Vicious walk related to the Green's function of TASEP. The height of the top layer gives the positions of particles. The dependence on the initial condition is reflected in the function  $\psi_j(x)$ .

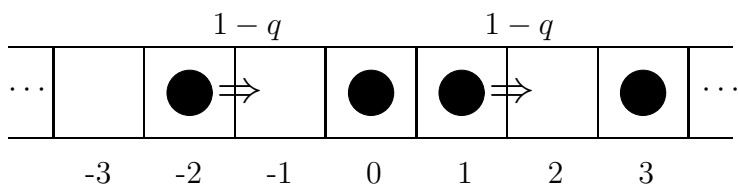


Figure 1

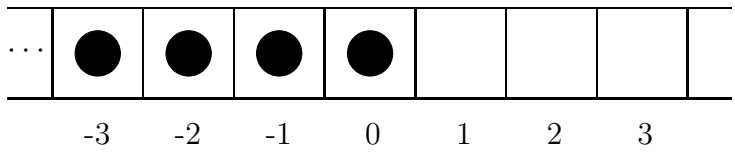


Figure 2

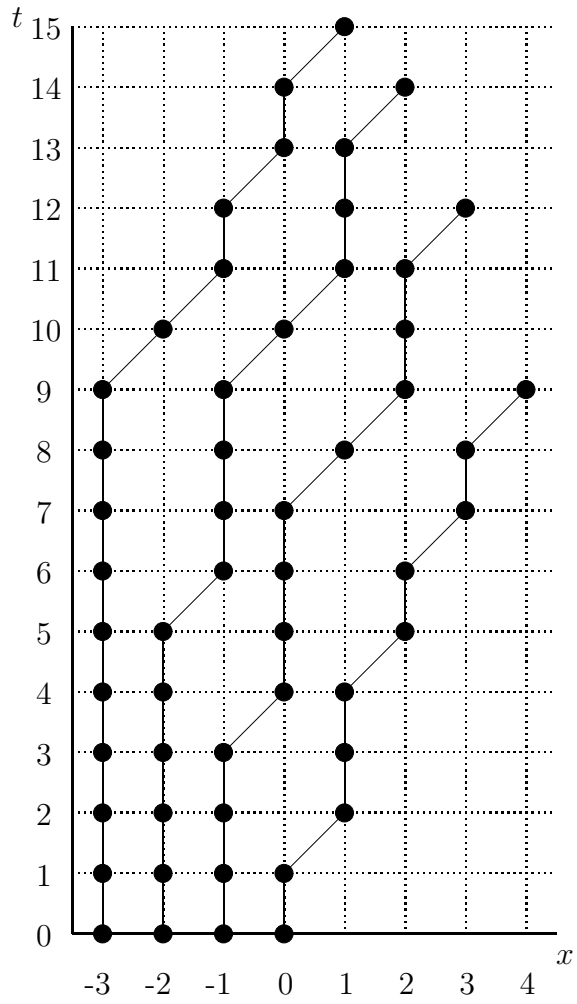


Figure 3

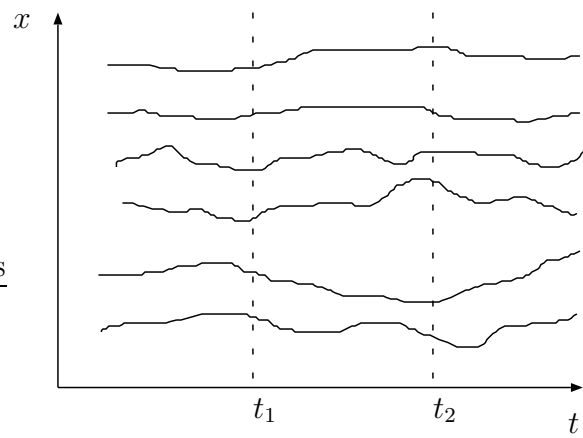


Figure 4

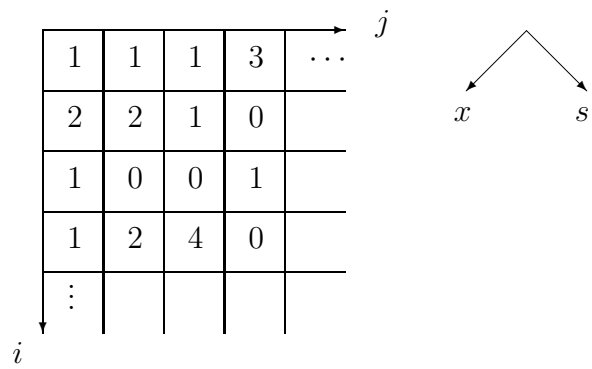


Figure 5

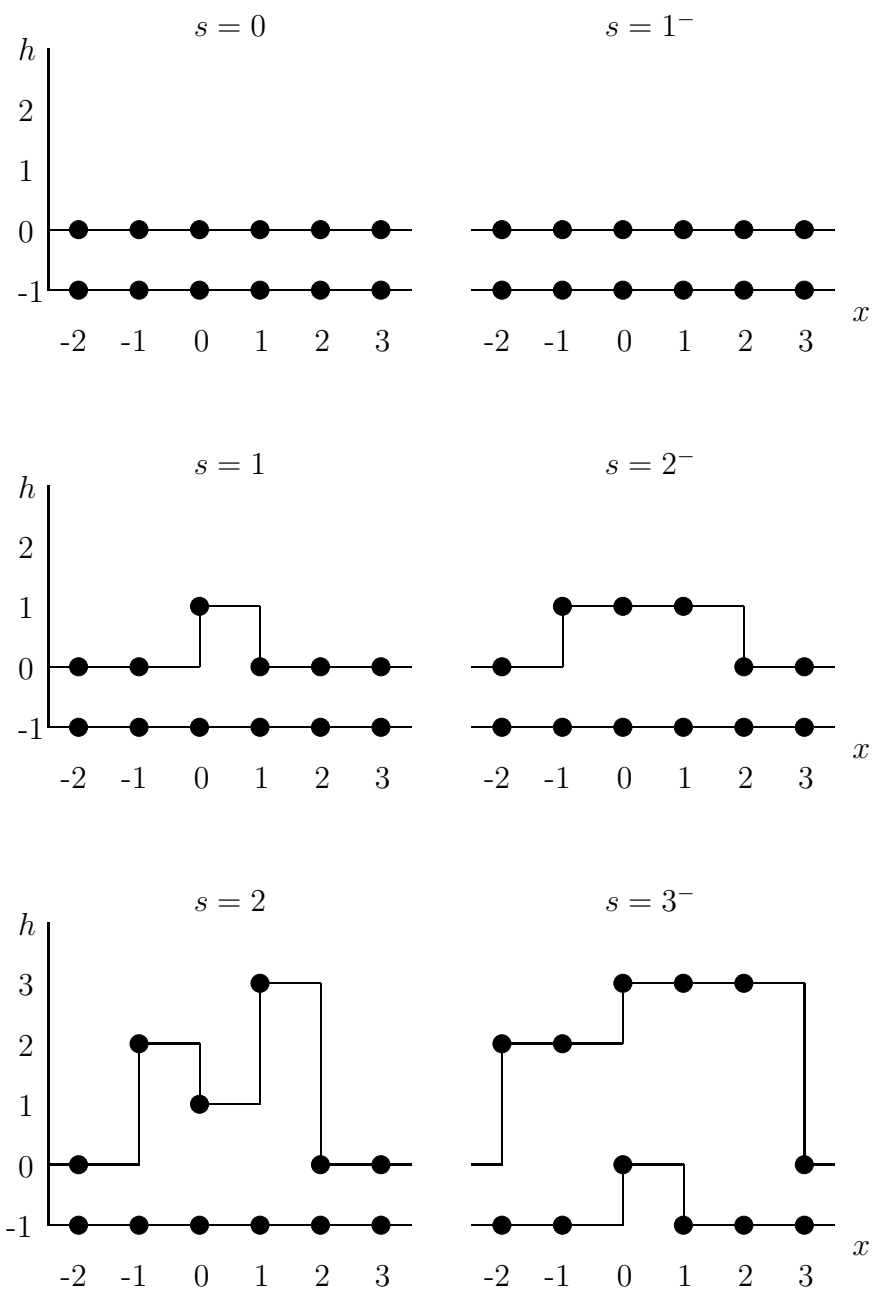


Figure 6

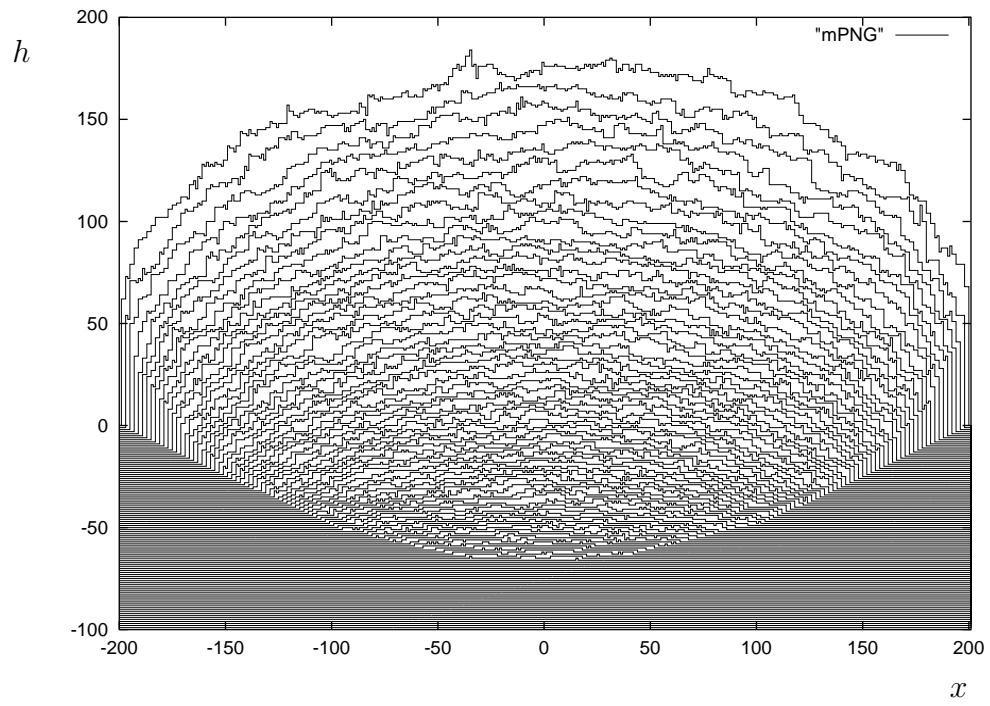


Figure 7

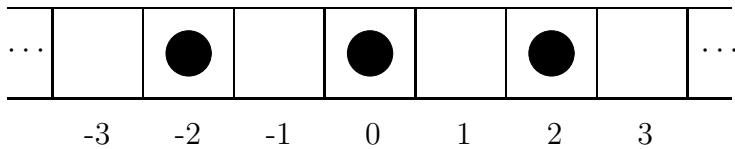


Figure 8

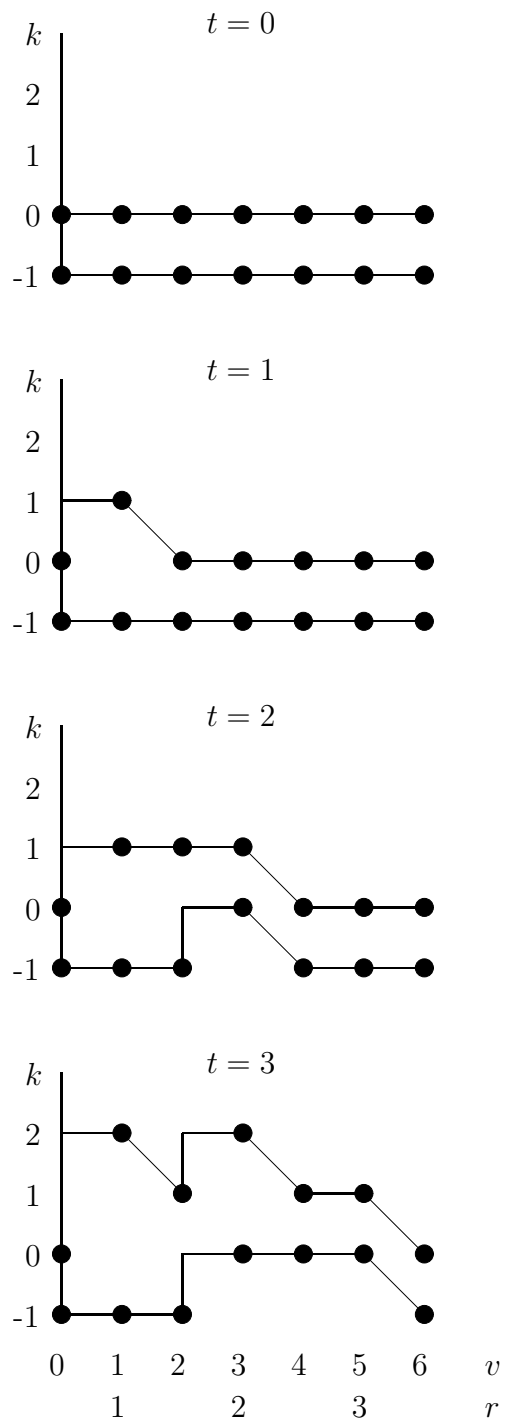


Figure 9

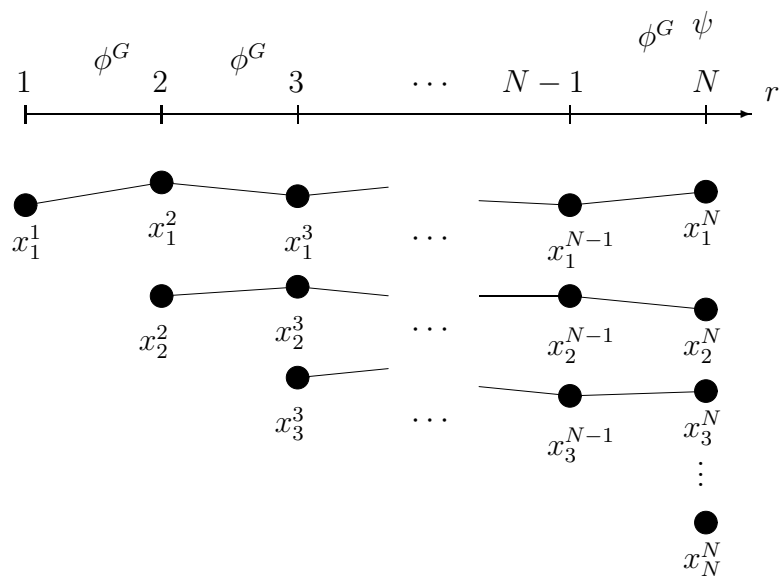


Figure 10